

# Quantum computing with spins in solids

W. A. Coish and Daniel Loss

27th August 2018

Department of Physics and Astronomy, University of Basel, Klingelbergstrasse  
82, CH-4056 Basel, Switzerland

## Abstract

The ability to perform high-precision one- and two-qubit operations is sufficient for universal quantum computation. For the Loss-DiVincenzo proposal to use single electron spins confined to quantum dots as qubits, it is therefore sufficient to analyze only single- and coupled double-dot structures, since the strong Heisenberg exchange coupling between spins in this proposal falls off exponentially with distance and long-ranged dipolar coupling mechanisms can be made significantly weaker. This scalability of the Loss-DiVincenzo design is both a practical necessity for eventual applications of multi-qubit quantum computing and a great conceptual advantage, making analysis of the relevant components relatively transparent and systematic. We review the Loss-DiVincenzo proposal for quantum-dot-confined electron spin qubits, and survey the current state of experiment and theory regarding the relevant single- and double- quantum dots, with a brief look at some related alternative schemes for quantum computing.

**Keywords:** quantum dots, quantum computing, single dot, double dot, decoherence, entanglement, quantum information processing, Coulomb blockade, stability diagram, encoded qubits, hyperfine interaction, spin-orbit interaction, relaxation, spin-echo

## 1 INTRODUCTION

Recent advances in semiconductor spintronics and, more specifically, spin-based quantum computing in solid-state systems, have encouraged significant research efforts in the last years (Prinz 1998, Wolf et al. 2001, Awschalom et al. 2002). Much of this research is motivated by pressure on the electronics industry to maintain Moore's-law growth in systems with components that are very quickly approaching the nanoscale, where quantum mechanics becomes important (ITRS 2005). Additionally, nanoscale devices provide a unique opportunity

to study the fundamental physics of quantum phenomena in a controllable environment.

Independent of the particular motivation, if quantum information processing is to progress beyond basic proof-of-principle experiments, it must be based on a viable, scalable qubit (a quantum mechanical two-level system, which can be placed in an arbitrary superposition of its basis states:  $|\psi\rangle = a|0\rangle + b|1\rangle$ ). The two states of single electron spins ( $|\uparrow\rangle = |0\rangle$  and  $|\downarrow\rangle = |1\rangle$ ), confined to semiconductor quantum dots (the Loss-DiVincenzo proposal), are one such qubit (Loss and DiVincenzo 1998). These qubits are viable, in the sense that they make use of fabrication techniques and electrical control concepts that have been developed over the last five decades in research laboratories and industry. The secret to scalability in the Loss-DiVincenzo proposal lies in local gating; this proposal would implement gating operations through the exchange interaction, which can be tuned locally with exponential precision, allowing pairs of neighboring qubits to be coupled and decoupled independently. This is to be contrasted with proposals that make use of long-ranged interactions (e.g., dipolar coupling) for which scalability may be called into question. The local, tunable nature of inter-qubit interactions in the Loss-DiVincenzo proposal is what makes it possible to consider first isolated one-qubit (single-quantum-dot), then isolated two-qubit (double-quantum-dot) systems. Once single- and double- quantum dots are understood, along with environmental coupling mechanisms, a quantum computation can proceed through a series of one- and two-qubit operations, without great concern regarding interactions between three, four, and more qubits.

There are many other proposals for qubits and associated quantum control processes. Some examples include various proposals that use superconducting devices (for reviews, see (Makhlin et al. 2001, Burkard 2004)), proposals for “adiabatic quantum computing”, in which quantum computations are performed through adiabatic manipulation of coupling constants in physically realizable Hamiltonians (Farhi et al. 2000, Farhi et al. 2001, Wu et al. 2005) (which might be used to perform fast quantum simulations of, e.g., superconducting pairing models (Wu et al. 2002)), electron spin qubits encoded in two-spin states (Levy 2002) or many-spin chains (Meier et al. 2003*b*, Meier et al. 2003*a*) (recent work showing that such spin chains can be built-up atom-by-atom on a surface (Hirjibehedin et al. 2006) is a possible first step to implementing such a proposal), cavity-QED schemes (Sleator and Weinfurter 1995, Domokos et al. 1995), trapped-ion proposals (Cirac and Zoller 1995), etc. Each of these proposals has advantages and disadvantages. Here we do not compare the relative merits of all proposals, but instead focus on proposals involving electron spins confined to quantum dots.

Before a quantum computation can begin, the qubits in a working quantum computer must be initialized to some state, e.g.  $|0\rangle$ . These qubits must be sufficiently isolated from the surrounding environment to reduce decoherence, there must be some way to perform fast single- and two-qubit operations in a time scale much less than the qubit decoherence time, and it must be possible to read out the final state of the qubits after any quantum computation (DiVincenzo 2000). In the following sections, we address these issues and others

which are important for the Loss-DiVincenzo proposal. In the process, we survey some recent work on quantum computing with electron spins in quantum dots.

Due to the rapid development of this field, there have been many recent reviews on quantum-dot quantum computing. Among these numerous reviews, there has been work that focuses on single-electron charge qubits in double dots (Fujisawa et al. 2006), the implementation of single-electron spin resonance (ESR), and the molecular wavefunctions of coupled double dots (van der Wiel et al. 2006), various proposals for spin-based quantum computing (Cerletti et al. 2005), silicon-based proposals for quantum computing (Koiller et al. 2005), general quantum computing in the solid state, including both quantum dots and superconducting systems (Burkard 2004), experiments and experimental proposals for quantum-dot-confined electrons (Engel et al. 2004a), the many coupling schemes and decoherence mechanisms for quantum-dot spin qubits (Hu 2004), and optical properties of quantum dots (Hohenester 2004). In this review, we analyze the Loss-DiVincenzo proposal from the viewpoint that this proposal can be decomposed into first single and then double quantum dots, with a special emphasis on double-dot physics.

This review is organized as follows: in Section 2 we give a brief summary of the Loss-DiVincenzo proposal for quantum computing. In Section 3 we discuss the characterization and manipulation of spin and charge states of electrons in single quantum dots. Section 4 contains a description of double quantum dots that emphasizes the single-electron regime, which is relevant for quantum-dot quantum computing. In Section 5 we survey important decoherence mechanisms for electron spins in single- and double- quantum dots. In Section 6 we briefly review some proposals for the generation and detection of nonlocal entanglement of electron spins in nanostructures, and in Section 7 we conclude with a brief summary of important topics for future study.

## 2 SPINS IN QUANTUM DOTS: AN OVERVIEW OF THE LOSS-DIVINCENZO PROPOSAL

In the original Loss-DiVincenzo proposal, the qubits are stored in the two spin states of single confined electrons. The considerations discussed in (Loss and DiVincenzo 1998) are generally applicable to electrons confined to any structure (e.g. atoms, molecules, defects, etc.), although the original proposal focused on applications in gated semiconductor quantum dots, as shown in Figure 1. Voltages applied to the top gates of such structures provide a confining potential for electrons in a two-dimensional electron gas (2DEG), below the surface. A negative voltage applied to a back-gate depletes the 2DEG locally, allowing the number of electrons in each dot to be reduced down to one (the single-electron regime). Advances in materials fabrication and gating techniques have now allowed for the realization of single electrons in single vertical (Tarucha et al. 1996) and gated lateral (Ciorga et al. 2000) dots, as well as double dots

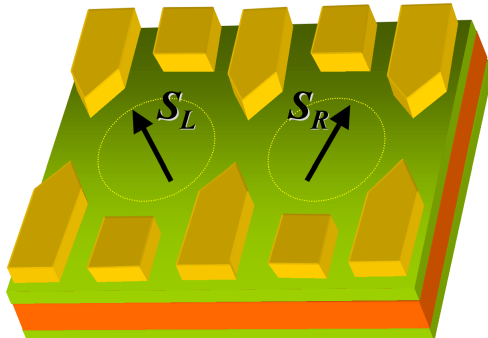


Figure 1: A double quantum dot. Top-gates are set to an electrostatic voltage configuration that confines electrons in the two-dimensional electron gas (2DEG) below to the circular regions shown. Applying a negative voltage to the back-gate, the dots can be depleted until they each contain only one single electron, each with an associated spin-1/2 operator  $\mathbf{S}_{L(R)}$  for the electron in the left (right) dot. The  $|\uparrow\rangle$  and  $|\downarrow\rangle$  spin-1/2 states of each electron provide a qubit (two-level quantum system).

(Elzerman et al. 2003, Hayashi et al. 2003, Petta et al. 2004).

Initialization of all qubits in the quantum computer to the Zeeman ground state  $|\uparrow\rangle = |0\rangle$  could be achieved by allowing all spins to reach thermal equilibrium at temperature  $T$  in the presence of a strong magnetic field  $B$ , such that  $|g\mu_B B| > k_B T$ , with  $g$ -factor  $g < 0$ , Bohr magneton  $\mu_B$ , and Boltzmann's constant  $k_B$  (Loss and DiVincenzo 1998). For further initialization schemes, see Section 3.2 below.

Once the qubits have been initialized to some state, they should remain in that state until a computation can be executed. In the absence of environmental coupling, the spins-1/2 of single electrons are intrinsic two-level systems, which cannot “leak” into higher excited states. Additionally, since electron spins only couple to charge degrees of freedom indirectly through the spin-orbit (or hyperfine) interactions, they are relatively immune to fluctuations in the surrounding electronic environment.

Single-qubit operations in the Loss-DiVincenzo quantum computer could be carried out by varying the Zeeman splitting on each dot individually (Loss and DiVincenzo 1998). It may be possible to do this through  $g$ -factor modulation (Salis et al. 2001), the inclusion of magnetic layers (Myers et al. 2005) (see also Figure 2), modification of the local Overhauser field due to hyperfine couplings (Burkard et al. 1999), or with nearby ferromagnetic dots (Loss and DiVincenzo 1998). There are a number of alternate methods that could be used to perform single-qubit rotations (see Section 3.2).

Two-qubit operations would be performed within the Loss-DiVincenzo proposal by pulsing the exchange coupling between two neighboring qubit spins

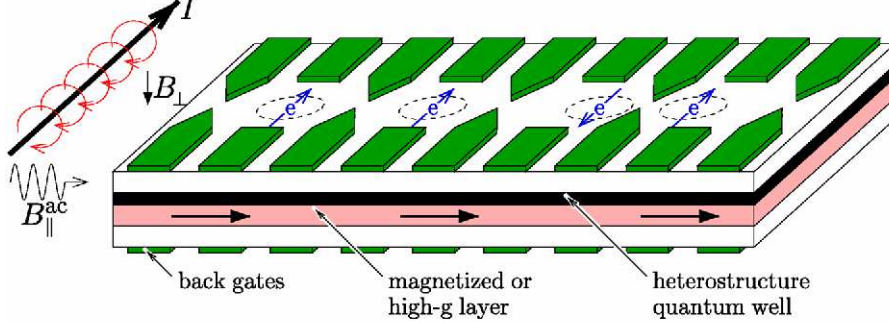


Figure 2: A series of exchange-coupled electron spins. Single-qubit operations could be performed in such a structure using electron spin resonance (ESR), which would require an rf transverse magnetic field  $B_{\perp}^{\text{ac}}$ , and a site-selective Zeeman splitting  $g(x)\mu_B B_{\perp}$ , which might be achieved through  $g$ -factor modulation or magnetic layers. Two-qubit operations would be performed by bringing two electrons into contact, introducing a nonzero wavefunction overlap and corresponding exchange coupling for some time (two electrons on the right). In the idle state, the electrons can be separated, eliminating the overlap and corresponding exchange coupling with exponential accuracy (two electrons on the left).

“on” to a non-zero value ( $J(t) = J_0 \neq 0$ ,  $t \in \{-\tau_s/2 \dots \tau_s/2\}$ ) for a switching time  $\tau_s$ , then switching it “off” ( $J(t) = 0$ ,  $t \notin \{-\tau_s/2 \dots \tau_s/2\}$ ). This switching can be achieved by briefly lowering a center-gate barrier between neighboring electrons, resulting in an appreciable overlap of the electron wavefunctions (Loss and DiVincenzo 1998), or alternatively, by pulsing the relative back-gate voltage of neighboring dots (Petta et al. 2005a) (see Section 4.3). Under such an operation (and in the absence of Zeeman or weaker spin-orbit or dipolar interactions), the effective two-spin Hamiltonian takes the form of an isotropic Heisenberg exchange term, given by (Loss and DiVincenzo 1998, Burkard et al. 1999)

$$H_{\text{ex}}(t) = J(t)\mathbf{S}_{\text{L}} \cdot \mathbf{S}_{\text{R}}, \quad (1)$$

where  $\mathbf{S}_{\text{L(R)}}$  is the spin-1/2 operator for the electron in the left (right) dot, as shown in Figure 1. The Hamiltonian  $H_{\text{ex}}(t)$  generates the unitary evolution  $U(\phi) = \exp[-i\phi\mathbf{S}_{\text{L}} \cdot \mathbf{S}_{\text{R}}]$ , where  $\phi = \int J(t)dt/\hbar$ . If the exchange is switched such that  $\phi = \int J(t)dt/\hbar = J_0\tau_s/\hbar = \pi$ ,  $U(\phi)$  exchanges the states of the two neighboring spins, i.e.:  $U(\pi)|\mathbf{n}, \mathbf{n}'\rangle = |\mathbf{n}', \mathbf{n}\rangle$ , where  $\mathbf{n}$  and  $\mathbf{n}'$  are two arbitrarily oriented unit vectors and  $|\mathbf{n}, \mathbf{n}'\rangle$  indicates a simultaneous eigenstate of the two operators  $\mathbf{S}_{\text{L}} \cdot \mathbf{n}$  and  $\mathbf{S}_{\text{R}} \cdot \mathbf{n}'$ .  $U(\pi)$  implements the so-called SWAP operation. If the exchange is pulsed on for the shorter time  $\tau_s/2$ , the resulting operation  $U(\pi/2) = (U(\pi))^{1/2}$  is known as the “square-root-of-SWAP” ( $\sqrt{\text{SWAP}}$ ). The  $\sqrt{\text{SWAP}}$  operation in combination with arbitrary single-qubit operations

is sufficient for universal quantum computation (Barenco et al. 1995*a*, Loss and DiVincenzo 1998). The  $\sqrt{\text{SWAP}}$  operation has now been successfully implemented in experiments involving two electrons confined to two neighboring quantum dots (as in Figure 1) (Petta et al. 2005*a*, Laird et al. 2005). Errors during the  $\sqrt{\text{SWAP}}$  operation have been investigated due to nonadiabatic transitions to higher orbital states (Schliemann et al. 2001, Requist et al. 2005), spin-orbit-interaction (Bonesteel et al. 2001, Burkard and Loss 2002, Stepanenko et al. 2003), and hyperfine coupling to surrounding nuclear spins (Petta et al. 2005*a*, Coish and Loss 2005, Klauser et al. 2005, Taylor et al. 2006). The isotropic form of the exchange interaction given in Equation (1) is not always valid. In realistic systems, a finite spin-orbit interaction leads to anisotropic terms which may cause additional errors, but could also be used to perform universal quantum computing with two-spin encoded qubits, in the absence of single-spin rotations (Bonesteel et al. 2001, Lidar and Wu 2002, Stepanenko and Bonesteel 2004, Chutia et al. 2006) (see also Section 4.4 below).

In the Loss-DiVincenzo proposal, readout could be performed using spin-to-charge conversion. This could be accomplished with a “spin filter” (spin-selective tunneling) to leads or a neighboring dot, coupled with single-electron charge detection (see also Section 3.2, below).

### 3 SINGLE QUANTUM DOTS

The fundamental element of information in a quantum computer is the quantum bit, or qubit. The qubits of the Loss-DiVincenzo proposal (Loss and DiVincenzo 1998) are encoded in the two spin states  $|\uparrow\rangle$  and  $|\downarrow\rangle$  of single electrons confined to quantum dots.

There are many different types of quantum dot that can be manufactured, each with distinct characteristics. Gated lateral quantum dots (as shown in Figures 1 and 2) offer the benefit that their shape and size can be controlled to suit a particular study, and the tunnel coupling between pairs of these dots can be tuned in a straightforward manner: by raising or lowering the barrier between the dots. Gated vertical dots (Tarucha et al. 1996) are created by etching surrounding material to form a pillar structure, with vertical confinement provided by a double-barrier heterostructure. Vertical dots allow for the controlled fabrication of quantum dots with large level spacing, although tunability of the coupling in these structures is restricted due to the fabrication process. To resolve this issue, hybrid laterally-coupled vertical double quantum dots have been manufactured, in which the inter-dot tunnel coupling is controllable (Hatano et al. 2005). Self-assembled quantum dots are yet another type of dot that can be used for quantum information processing. Self-assembled dots form spontaneously during epitaxial growth due to a lattice mismatch between the dot and substrate materials. These dots can be made with very large single-particle level spacings, but typically form at random locations, which makes controlled coupling through a tunnel junction difficult. Such dots can, however, potentially be coupled with optical cavity modes (Imamoğlu et al. 1999),

and new techniques have now allowed the fabrication of cavities with modes that couple maximally directly at the positions of isolated dots (Badolato et al. 2005).

In the rest of this section we focus on lateral quantum dots, as shown in Figures 1 and 2. After a brief review of charge and spin control in single quantum dots, we will address issues specific to double quantum dots in Section 4.

### 3.1 Charge control: Coulomb blockade

To ensure a single two-level system is available to be used as a qubit, it is practical to consider single isolated electron spins (with intrinsic spin  $1/2$ ) confined to single orbital levels. A natural first step to implementing the Loss-DiVincenzo proposal was therefore to demonstrate control over the charging of a quantum dot electron-by-electron in a single gated quantum dot. This is typically done by operating a quantum dot in the Coulomb-blockade regime, where the energy for the addition of an electron to the quantum dot is larger than the energy that can be supplied by electrons in the source or drain leads. In this case, the charge on the quantum dot is conserved, and no electrons can tunnel onto or off of the dot. For a general review of Coulomb blockade phenomena and the characterization of many-electron states in single quantum dots, see (Kouwenhoven et al. 2001).

### 3.2 Spin control: Initialization, operations, and readout.

As mentioned in Section 2, initialization of all electron spins to the “up” state  $|\uparrow\rangle$  could be achieved by allowing all spins to equilibrate in a strong magnetic field. Depending on the particular architecture, this may take a long time or it may be inconvenient to have large magnetic fields in the region of the apparatus. Initialization could also be achieved through spin-injection from a ferromagnet, as has been performed in bulk semiconductors (Fiederling et al. 1999, Ohno et al. 1999), with a spin-polarized current from a spin-filter device (Prinz and Hathaway 1995, Prinz 1998, Loss and DiVincenzo 1998, DiVincenzo 1999, Recher et al. 2000), or by optical pumping (Cortez et al. 2002, Shabaev et al. 2003, Gywat et al. 2004, Bracker et al. 2005), which has now allowed the preparation of spin states with very high fidelity, in one case as high as 99.8% (Atature et al. 2006).

Single-qubit operations can be performed in the Loss-DiVincenzo proposal whenever the Zeeman energy of the quantum-dot spins can be tuned locally, as mentioned in Section 2. Alternative single-qubit-rotation schemes may require global magnetic field gradients (Wu et al. 2004, Tokura et al. 2006), ESR (see Figure 2) or, in the presence of spin-orbit interaction, electric-dipole spin resonance (EDSR) techniques. EDSR has been analyzed in great detail for two-dimensional systems in theory (Rashba and Efros 2003, Duckheim and Loss 2006) and experiment (Kato et al. 2004), and can also be applied to lower-dimensional systems (quantum wires and quantum dots) (Levitov and Rashba 2003, Golovach et al. 2006), with the advantage that single-qubit operations could then be performed using fast all-electrical control. New experiments

have now shown that it may be possible in practice to perform single-spin operations on single quantum dots using ESR, as depicted in Figure 2 (Koppens et al. 2006).

As mentioned in Section 2, quantum-dot spin readout can be performed using a spin filter. Experimentally, spin filters have been reported in the open (Potok et al. 2002) and Coulomb-blockade regimes (Folk et al. 2003), and have even been used to determine the longitudinal spin decay ( $T_1$ ) time (Hanson et al. 2003, Hanson et al. 2004) using an  $n$ -shot readout scheme, which has been analyzed in detail (Engel et al. 2004b). A single-shot readout has also been demonstrated (Elzerman et al. 2004) and improved upon (Hanson et al. 2005). Non-invasive readout schemes using spin-to-charge conversion and quantum-point-contact (QPC) measurements have been used on two-spin encoded qubits (Johnson et al. 2005a, Petta et al. 2005a, Petta et al. 2005b, Johnson et al. 2005b).

To measure the transverse spin coherence time  $T_2$ , there have been proposals to perform ESR and detect the resulting resonance in stationary current (Engel and Loss 2001), changes in the resistivity of a neighboring field-effect transistor (FET) (Martin et al. 2003), optically (Gywat et al. 2004), or from current noise (Schaefer and Strunz 2005). ESR in single quantum dots has not yet been observed, in part because it is challenging to generate high-frequency magnetic fields with sufficient power for single-spin manipulation without “heating” electrons on the quantum dot or in the surrounding leads through the associated electric field (van der Wiel et al. 2006). Recent experiments that employ a double quantum dot in the spin-blockade regime may have overcome this problem (Koppens et al. 2006) (see also the discussion on spin blockade near the end of Section 5 below).

## 4 DOUBLE QUANTUM DOTS

Single qubits are the fundamental unit of quantum information in quantum computing. However, universal quantum computation still requires both single-qubit and two-qubit operations (Barenco et al. 1995b). In the Loss-DiVincenzo proposal, two-qubit gates are performed with exchange-coupled electron spins confined to two neighboring quantum dots (double dots). Double dots are also important for encoded qubits (Levy 2002), in which qubits are encoded into a two-dimensional pseudospin-1/2 subspace of a four-dimensional two-electron spin system.

In this section we discuss characterization and manipulation techniques that are commonly used to extract microscopic parameters of double quantum dots. In Section 4.1 we review the charge stability diagram, and illustrate its connection to a commonly used microscopic model Hamiltonian. In Section 4.2 we review work on the coherent coupling of double quantum dots, which is required to generate a large exchange interaction for two-qubit gating. In Section 4.3 we discuss the use of double quantum dots as two-qubit gates, and in Section 4.4 we review some work on using double quantum dots to control



single “encoded” qubits (Levy 2002), a topic which has now come into vogue (Petta et al. 2005*a*, Taylor et al. 2005, Burkard and Imamoglu 2006, Hanson and Burkard 2006).

### 4.1 The double-dot charge stability diagram

Just as transport through a single quantum dot and Coulomb blockade phenomena give information about the orbital level spacing, charging energy, and spin states of single quantum dots, similar studies can be carried-out on double quantum dots. Whereas for single dots, transport phenomena are typically understood in terms of one-dimensional plots of conductance versus gate voltage, the primary tool used to understand double quantum dots is the double-dot charge stability diagram. The stability diagram is a two-dimensional plot of current or differential conductance through the double dot or through a neighboring QPC, given as a function of two independent back-gate voltages (one applied locally to each dot). The plot differentiates regions where the double-dot ground state has a charge configuration  $(N_1, N_2)$ , for various  $N_1, N_2$ , where  $N_1$  is the number of charges on the left dot and  $N_2$  is the number of charges on the right. Transport through double quantum dots and the relevant charge stability diagram has been discussed thoroughly in (van der Wiel et al. 2003). In the rest of this section, we review some features of the double-dot stability diagram with an emphasis on the connection to a model Hamiltonian that is commonly used in the literature (Klimeck et al. 1994, Pals and MacKinnon 1996, Golden and Halperin 1996, Ziegler et al. 2000).

An isolated double quantum dot is described by the Hamiltonian

$$H_{\text{dd}} = H_C + H_T + H_S, \quad (2)$$

where  $H_C$  gives the single-particle and inter-particle charging energies as well as the orbital energy,  $H_T$  is the inter-dot tunneling term due to a finite overlap of dot-localized single-particle wavefunctions, which ultimately gives rise to exchange, and  $H_S$  contains explicitly spin-dependent terms, which may include spin-orbit interaction, dipole-dipole interaction, and the contact hyperfine interaction between the confined electron spins and nuclear spins in the surrounding lattice.

There are several approaches that can be taken to writing the various components of the double-dot Hamiltonian  $H_{\text{dd}}$ , corresponding to several degrees of microscopic detail. In the simplest form, the Hubbard model, details of the electron wavefunctions are neglected and the Coulomb interaction is given only in terms of on-site and nearest-neighbor terms. Since this description relies only on very few parameters, it is the most commonly used in the literature on transport phenomena through quantum dots. The shape of the confining potential, quantum-dot localized wavefunctions, and form of the Coulomb interaction may become important in certain circumstances, in which case it is more appropriate to apply either the Heitler-London method (which neglects doubly-occupied dot levels), or the Hund-Mulliken method, which includes the

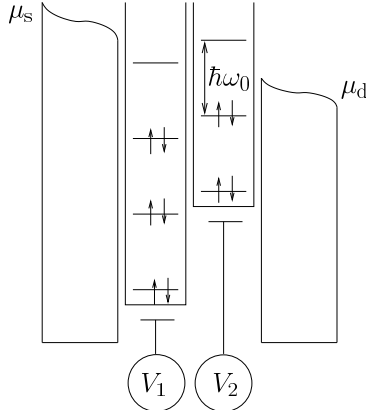


Figure 3: Ground-state configuration for a double quantum dot with large orbital and charging energies, and negligible dot-lead and interdot coupling.  $\mu_{s(d)}$  is the source (drain) chemical potential,  $V_{1(2)}$  is the left (right) local dot potential, which is related to applied gate potentials by a linear transformation (see Equation (5), below), and both dots are assumed to have the same uniform level spacing  $\hbar\omega_0$ .

effects of double-occupancy. These methods predict, for instance, a variation of the interdot exchange interaction through zero with increasing out-of-plane magnetic field (Burkard et al. 1999). Experimentally, it has been confirmed that the exchange coupling can be tuned with an out-of-plane magnetic field in single vertical (Fujisawa et al. 2002) and single lateral quantum dots (Zumbühl et al. 2004), which behave effectively as double-dot structures. Here we ignore these effects and focus on the simplest Hubbard model that reproduces much of the double-dot physics that can be seen in transport phenomena.

We model the Coulomb interaction with simple on-site ( $U_{1(2)}$  for the left (right) dot) and nearest-neighbor ( $U'$ ) repulsion. The single-particle charging energy is given in terms of a local dot potential  $V_{1(2)}$ . The charging Hamiltonian is then

$$H_C = \frac{1}{2} \sum_l U_l N_l (N_l - 1) + U' N_1 N_2 - |e| \sum_l V_l N_l + \sum_{kl} \epsilon_{lk} n_{lk}, \quad (3)$$

where  $N_l = \sum_k n_{lk}$  counts the total number of electrons in dot  $l$ , with  $n_{lk} = \sum_\sigma d_{lk\sigma}^\dagger d_{lk\sigma}$ , and here  $d_{lk\sigma}$  annihilates an electron on dot  $l$ , in orbital  $k$ , with spin  $\sigma$ .  $\epsilon_{lk}$  is the energy of single-particle orbital level  $k$  in dot  $l$ , which gives rise to the typical orbital level spacing  $\epsilon_{lk+1} - \epsilon_{lk} \approx \hbar\omega_0$  (see Figure 3).

Within the capacitive charging model described by the equivalent circuit in the inset of Figure 4(a), the microscopic charging energies are related to

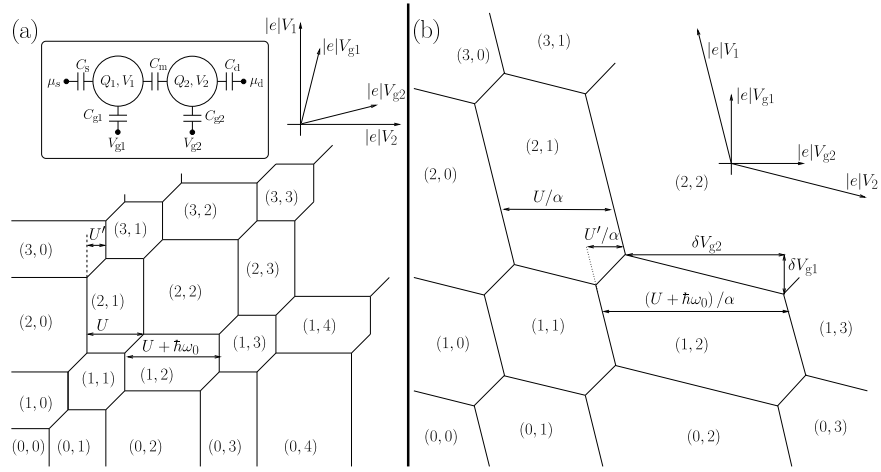


Figure 4: Stability diagram plotted in terms of (a) local dot potentials  $V_{1,2}$  and (b) applied gate potentials  $V_{g1,2}$ , with on-site charging energies  $U_l = U$ ,  $l = 1, 2$ , nearest-neighbor charging energy  $U'$ , and dot orbital level spacing  $\hbar\omega_0$  satisfying  $U : \hbar\omega_0 : U' = 3 : 2 : 1$ . In addition, for (b) we have assumed the voltage scaling factors are the same for both dots, and are given by  $\alpha_1 = \alpha_2 = \alpha = 1/2$ . (a) inset: capacitive charging model for a double quantum dot, indicating the source (drain) chemical potential  $\mu_{s(d)}$ , the charge on the left (right) dot  $Q_{1(2)}$ , the capacitances to source (drain)  $C_{s(d)}$ , the mutual capacitance  $C_m$ , and gate capacitances  $C_{g1,2}$ . (b) Horizontal lines in the  $|e|V_{1(2)}$  plane become skewed with slope  $\delta V_{g1}/\delta V_{g2} = -C_1 C_{g2}/C_m C_{g1}$  when plotted versus  $|e|V_{g1(2)}$ .

capacitances by (Ziegler et al. 2000, van der Wiel et al. 2003)

$$U_l = \frac{C_1 C_2}{C_1 C_2 - C_m^2} \frac{e^2}{C_l}, \quad U' = \frac{2e^2 C_m}{C_1 C_2 - C_m^2}, \quad (4)$$

where  $C_1 = C_s + C_m + C_{g1}$ ,  $C_2 = C_d + C_m + C_{g2}$ , and all capacitances are defined in the inset of Figure 4(a). In experiments, the local quantum dot potentials  $V_{1,2}$  are controlled indirectly in terms of gate voltages  $V_{g1,2}$ , which are capacitively coupled to the dots through gate capacitances  $C_{g1,2}$ . For fixed quantum-dot charges  $(Q_1, Q_2) = -|e|(N_1, N_2) = \text{const.}$ , differences in the dot voltages  $\Delta V_1$  and  $\Delta V_2$  are related to differences in the gate voltages  $\Delta V_{g1}$  and  $\Delta V_{g2}$  through (Ziegler et al. 2000, van der Wiel et al. 2003)

$$\begin{pmatrix} C_1 & -C_m \\ -C_m & C_2 \end{pmatrix} \begin{pmatrix} \Delta V_1 \\ \Delta V_2 \end{pmatrix} = \begin{pmatrix} C_{g1} \Delta V_{g1} \\ C_{g2} \Delta V_{g2} \end{pmatrix}. \quad (5)$$

The double-dot stability diagram can then be given equivalently as a two-dimensional plot with energy axes  $|e|V_1$ ,  $|e|V_2$ , or with axes  $|e|V_{g1}$ ,  $|e|V_{g2}$ , which are skewed and stretched with respect to the original axes according to the transformation given in Equation (5). The end effect is that parallel horizontal (vertical) lines in the  $|e|V_{1(2)}$  plane separated by a distance  $dV_{2(1)}$  transform to skewed parallel lines, separated by  $dV_{g2(1)} = dV_{2(1)}/\alpha_{2(1)}$  along the horizontal (vertical) of the new coordinate system, where (see Figure 4):

$$\alpha_l = \frac{C_{gl}}{C_l}, \quad l = 1, 2. \quad (6)$$

Additionally, horizontal lines in the  $|e|V_{1(2)}$  plane become skewed with a slope  $\delta V_{g1}/\delta V_{g2} = -C_m C_{g2}/C_2 C_{g1}$  (see Figure 4(b)), and vertical lines are skewed with slope  $\delta V_{g1}/\delta V_{g2} = -C_1 C_{g2}/C_m C_{g1}$ .

The Hamiltonian in Equation (3) conserves the number of electrons on each dot:  $[H_C, N_l] = 0$ , so we label the ground state by the two dot occupation numbers,  $(N_1, N_2)$ , and indicate where each configuration is the ground state in Figure 4 for equivalent quantum dots that satisfy  $\alpha_1 = \alpha_2 = \alpha = 1/2$ ,  $U_1 = U_2 = U$ ,  $\epsilon_{lk+1} - \epsilon_{lk} = \hbar\omega_0$  for all  $k, l$ , and  $U : \hbar\omega_0 : U' = 3 : 2 : 1$ . The charge stability diagram produces a ‘‘honeycomb’’ of hexagons with dimensions that are determined by three typical energy scales: (1) The on-site repulsion  $U$ , (2) the nearest-neighbor repulsion  $U'$ , and (3) the typical orbital energy  $\hbar\omega_0$ . Figure 4 assumes a ground-state electron filling as shown in Figure 3, with constant orbital energy  $\hbar\omega_0$ . In this case, the orbital energy appears in the dimensions of only every second honeycomb cell of the stability diagram, along the horizontal or vertical direction, since the spin-degenerate orbital states fill with two electrons at a time according to the Pauli principle. This even-odd behavior may not be visible in dots of high symmetry, where the orbital levels are manifold degenerate. Alternatively, the absence of an even-odd effect in low-symmetry single dots has previously been attributed to the absence of spin degeneracy due to many-body effects (Stewart et al. 1997, Fujisawa et al. 2001, van der Wiel et al. 2003).

Each vertex of a honeycomb cell corresponds to a triple-point, where three double-dot charge states are simultaneously degenerate. For a double dot connected to source and drain leads at low temperature, and in the absence of relaxation or photo-assisted tunneling processes, it is only at these points where resonant sequential transport can occur, through shuttling processes of the form  $(0,0) \rightarrow (1,0) \rightarrow (0,1) \rightarrow (0,0)$ . This picture changes when a strong inter-dot tunnel coupling  $H_T$  is considered in addition.

## 4.2 Molecular states in double dots

Molecule-like states have been observed and studied in detail in two-electron single vertical (Fujisawa et al. 2002) and lateral quantum dots (Zumbühl et al. 2004) (the latter behave as an effective double-dot structure, showing good agreement with theory (Golovach and Loss 2004)). Evidence of molecular states forming in double quantum dots due to a strong inter-dot tunnel-coupling has also been found in a variety of systems (Schmidt et al. 1997, Schedelbeck et al. 1997, Blick et al. 1998, Brodsky et al. 2000, Bayer et al. 2001, Ota et al. 2005, Hüttel et al. 2005, Fasth et al. 2005, Mason et al. 2004, Biercuk et al. 2005, Graeber et al. 2006). For example, molecular states have been observed in many-electron gated quantum dots in linear transport (Blick et al. 1998) (solid lines of Figure 5(b)) and transport through excited states (Hüttel et al. 2005) (dashed lines in Figure 5(b)). In addition, molecular states have been observed in vertical-lateral gated double quantum dots (Hatano et al. 2005), gated dots formed in quantum wires (Fasth et al. 2005) and gated carbon-nanotube double dots (Mason et al. 2004, Biercuk et al. 2005, Graeber et al. 2006). A large inter-dot tunnel coupling is essential for generating a large exchange interaction  $J$ , and is therefore very important for the implementation of fast two-qubit gates in the Loss-DiVincenzo proposal.

In this section, we analyze changes to the double-dot stability diagram that occur due to the inter-dot tunneling term  $H_T$ . We focus on the relevant regime for quantum computing, where only a single orbital state is available for occupation on each quantum dot (the lower-left region of Figures 4(a,b)). In the subspace of these lowest dot orbital states,  $H_T$  is given by:

$$H_T = \sum_{\sigma} t_{12} d_{1\sigma}^{\dagger} d_{2\sigma} + \text{H.c.}, \quad (7)$$

where  $t_{12}$  is the tunneling amplitude between the two dots, and  $d_{l\sigma}$ ,  $l = 1, 2$ , annihilates an electron in the lowest single-particle orbital state localized on quantum dot  $l$  with spin  $\sigma$ .

When the double dot is occupied by only  $N = 0, 1$  electrons and is coupled weakly to leads, an explicit expression can be found for the current passing through a sequentially-coupled double dot, as shown in Figure 5(a) (Ziegler et al. 2000, Graeber et al. 2006). It is straightforward to diagonalize  $H_C + H_T$  in the subspace of  $N = 1$  electrons on the quantum dot. This gives the (spin-

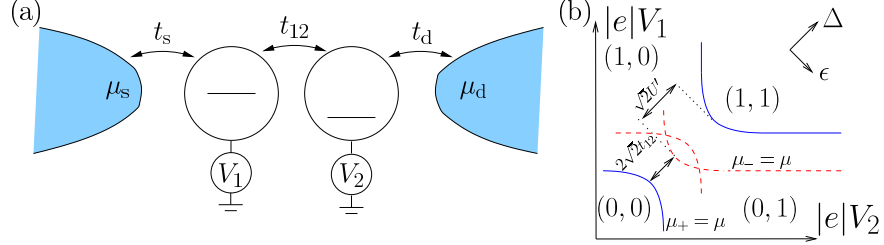


Figure 5: (a) A tunnel-coupled double quantum dot, with tunneling amplitude  $t_{12}$ . The source and drain leads, at chemical potentials  $\mu_s$  and  $\mu_d$ , are connected to the left and right dots through tunnel barriers with tunneling amplitudes  $t_s$  and  $t_d$ , respectively. The left and right dots are set to local potentials  $V_1$  and  $V_2$ . (b) Modification of the stability diagram in the case of a significant tunnel coupling  $t_{12}$ . To generate this figure we have chosen the ratio of tunnel coupling to the mutual (nearest-neighbor) charging energy to be  $t_{12}/U' \approx 1/5$ . At solid lines, transport occurs via the double-dot ground state  $|E_+\rangle$  and at dashed lines, additional transport can occur through the first excited state  $|E_-\rangle$  (see Equations (9) and (10) below).

degenerate) eigenenergies and corresponding eigenvectors:

$$E_{\pm}(\Delta, \epsilon) = -\frac{1}{\sqrt{2}} \left( \Delta \pm \sqrt{\epsilon^2 + 2t_{12}^2} \right), \quad (8)$$

$$|E_{\pm}\rangle = \cos\left(\frac{\theta_{\pm}}{2}\right) |1,0\rangle + \sin\left(\frac{\theta_{\pm}}{2}\right) |0,1\rangle, \quad (9)$$

$$\tan\left(\frac{\theta_{\pm}}{2}\right) = \frac{\epsilon}{\sqrt{2}t_{12}} \pm \sqrt{1 + \left(\frac{\epsilon}{\sqrt{2}t_{12}}\right)^2}. \quad (10)$$

Here,  $E_{\pm}(\Delta, \epsilon)$  is written in terms of new energy coordinates  $\epsilon, \Delta$ , which are related to the old (voltage) coordinates through a rotation of the axes by  $45^\circ$  (see also Figure 5(b)):

$$\begin{pmatrix} \Delta \\ \epsilon \end{pmatrix} = \frac{1}{\sqrt{2}} \begin{pmatrix} 1 & 1 \\ -1 & 1 \end{pmatrix} \begin{pmatrix} |e|V_1 \\ |e|V_2 \end{pmatrix}. \quad (11)$$

We then define double-dot chemical potentials:

$$\mu_{\pm}(\Delta, \epsilon) = E_{\pm}(\Delta, \epsilon) - E_0, \quad (12)$$

where  $E_0 = 0$  is the energy of the  $(0,0)$  charge configuration. In the presence of a strong tunnel coupling, the eigenstates of the double dot are no longer labeled separately by the quantum numbers  $N_1, N_2$ . Instead, the sum  $N = N_1 + N_2$  is conserved. If we add to  $H_{\text{dd}}$  the double-dot-lead coupling

Hamiltonian  $H_{\text{dd-L}} = \sum_{k\sigma} t_s c_{sk\sigma}^\dagger d_{1\sigma} + t_d c_{dk\sigma}^\dagger d_{2\sigma} + \text{H.c.}$ , where  $c_{s(d)k\sigma}^\dagger$  creates an electron in the source (drain), in orbital  $k$  with spin  $\sigma$ , then  $N$  can fluctuate between 1 and 0 if the double-dot and lead chemical potentials are equal. We identify double-dot sequential tunneling processes as those that change the total charge on the double dot by one:  $N \rightarrow N \pm 1$  (Golovach and Loss 2004). One can evaluate golden-rule rates for all sequential-tunneling processes, taking the dot-lead coupling  $H_{\text{dd-L}}$  as a perturbation to obtain the stationary current from a standard Pauli master equation (the Pauli master equation is valid for sufficiently high temperature,  $k_B T > \Gamma_{s(d)}$ , so that off-diagonal elements can be ignored in the double-dot density matrix). For weak dot-lead coupling, at low temperature  $k_B T < \hbar\omega_0$ , and at zero bias ( $\mu = \mu_s = \mu_d + \Delta\mu$ , with  $\Delta\mu \rightarrow 0$ ), transport occurs only through the  $N = 1$  ground state, with chemical potential  $\mu_+$ . The differential conductance near the  $N = 0, 1$  boundary is then given by

$$\frac{dI}{d(\Delta\mu)} = |e|\Gamma \left( \frac{-2f'(\mu_+)}{1+f(\mu_+)} \right), \quad \Gamma = \frac{\sin^2(\theta_+) \Gamma_s \Gamma_d}{4 \left( \cos^2\left(\frac{\theta_+}{2}\right) \Gamma_s + \sin^2\left(\frac{\theta_+}{2}\right) \Gamma_d \right)}, \quad (13)$$

where  $f(E) = 1 / \left[ 1 + \exp\left(\frac{E-\mu}{k_B T}\right) \right]$  is the Fermi function at chemical potential  $\mu$  and temperature  $T$ ,  $f'(E) = df(E)/dE$ , and  $\Gamma_{s(d)} = \frac{2\pi\nu}{\hbar} |t_{s(d)}|^2$  is the tunneling rate to the source (drain) with a lead density of states per spin  $\nu$  at the Fermi energy. If spin degeneracy is lifted, the quantity in brackets in Equation (13) is replaced by the familiar term  $-f'(\mu_+) = 1 / \left[ 4k_B T \cosh^2\left(\frac{\mu_+ - \mu}{2k_B T}\right) \right]$  (Beenakker 1991). The differential conductance (Equation (13)) reaches a maximum near the point where the double-dot chemical potential matches the lead chemical potential,  $\mu_+(\Delta, \epsilon) = \mu$ , which we indicate with a solid line in Figure 5(b). Transport through the excited state can occur where  $\mu_-(\Delta, \epsilon) = \mu$ , and when the bias  $\Delta\mu = \mu_s - \mu_d$  or temperature  $T$  are sufficiently large to generate a significant population in the excited state  $|E_-\rangle$ . Dashed lines indicate where  $\mu_-(\Delta, \epsilon) = \mu$  in Figure 5(b).

There are several qualitative changes to the double-dot stability diagram that take place in the presence of strong tunnel coupling. First, the number of electrons on each dot is not conserved individually. Instead, the sum  $N = N_1 + N_2$  is conserved, which means that there are no longer lines separating, for example, the (1,0) and (0,1) states in Figure 5(b). Second, sequential-tunneling processes allow current to be transported through the double-dot along the length of the ‘‘wings’’ that define the boundaries between  $N$  and  $N \pm 1$ -electron ground states. This is in contrast to the case where  $t_{12}$  is weak, in which resonant sequential transport can only occur at triple points, where the shuttling processes of the type  $(0, 0) \rightarrow (1, 0) \rightarrow (0, 1) \rightarrow (0, 0)$  are allowed by energy conservation.

### 4.3 Double dots as two-qubit gates

The  $\sqrt{\text{SWAP}}$  operation described in Section 2 requires significant control of the exchange coupling  $J$ . The value of  $J$  can be controlled by raising/lowering the

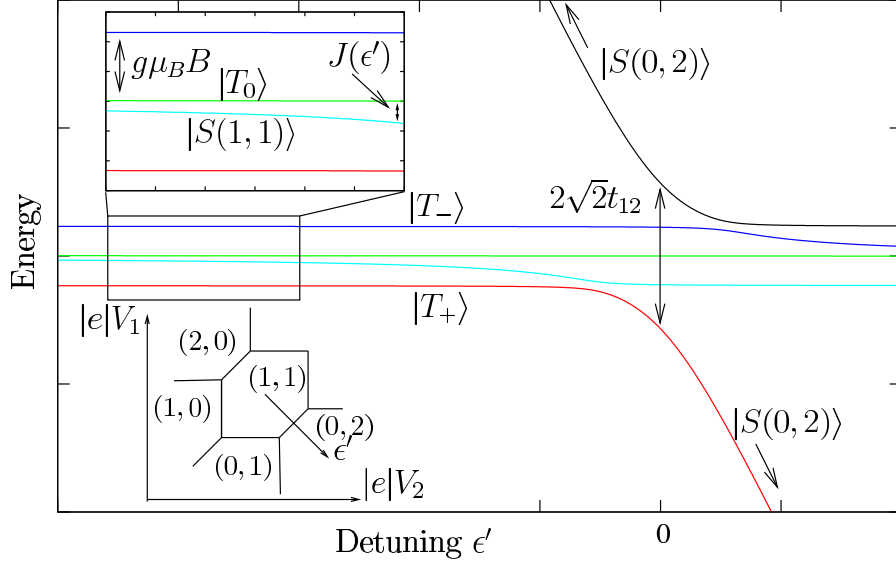


Figure 6: Energy-level spectrum for two electrons in a double quantum dot.

inter-dot barrier, thus changing the tunnel coupling  $t_{12}$  (Loss and DiVincenzo 1998), or with an out-of-plane magnetic field or weak in-plane electric field (Burkard et al. 1999). More recently, experiments have controlled  $J$  by varying the back-gate voltages on two neighboring quantum dots through a large parameter regime, independently (Petta et al. 2005*a*). Here we discuss this last method to control  $J$ , which has been analyzed in several recent papers (Petta et al. 2005*b*, Coish and Loss 2005, Taylor et al. 2006, Stopa and Marcus 2006).

We consider a double quantum dot in the region of the charge stability diagram indicated in the lower inset of Figure 6. Specifically, we consider the regime of gate voltages where the double dot contains  $N = 2$  electrons near the degeneracy point of the  $(1, 1)$  and  $(0, 2)$  charge states, and aim to diagonalize the Hamiltonian  $H_C + H_T$  in the basis of three spin triplets and two relevant singlets:

$$|S(0, 2)\rangle = d_{2\downarrow}^\dagger d_{2\uparrow}^\dagger |\text{vac.}\rangle, \quad (14)$$

$$|S(1, 1)\rangle = \frac{1}{\sqrt{2}} (d_{2\downarrow}^\dagger d_{1\uparrow}^\dagger - d_{2\uparrow}^\dagger d_{1\downarrow}^\dagger) |\text{vac.}\rangle, \quad (15)$$

$$|T_0\rangle = \frac{1}{\sqrt{2}} (d_{2\downarrow}^\dagger d_{1\uparrow}^\dagger + d_{2\uparrow}^\dagger d_{1\downarrow}^\dagger) |\text{vac.}\rangle, \quad (16)$$

$$|T_+\rangle = d_{2\uparrow}^\dagger d_{1\uparrow}^\dagger |\text{vac.}\rangle, \quad (17)$$

$$|T_-\rangle = d_{2\downarrow}^\dagger d_{1\downarrow}^\dagger |\text{vac.}\rangle. \quad (18)$$

In the absence of additional spin-dependent terms, the triplets are degenerate,



with energy  $E_{\text{Triplet}} = E_{(1,1)} = -\sqrt{2}\Delta'$ , whereas the two singlet states have energies and associated eigenvectors

$$E_{\text{Singlet}}^{\pm} = E_{\text{Triplet}} - \frac{1}{\sqrt{2}} \left( \epsilon' \pm \sqrt{(\epsilon')^2 + 4t_{12}^2} \right), \quad (19)$$

$$|E_{\text{Singlet}}^{\pm}\rangle = \cos\left(\frac{\theta_{\pm}^S}{2}\right) |S(1,1)\rangle + \sin\left(\frac{\theta_{\pm}^S}{2}\right) |S(0,2)\rangle, \quad (20)$$

$$\tan\left(\frac{\theta_{\pm}^S}{2}\right) = \frac{\epsilon'}{2t_{12}} \pm \sqrt{1 + \left(\frac{\epsilon'}{2t_{12}}\right)^2}. \quad (21)$$

Here,  $\Delta'$  and  $\epsilon'$  are related to the previous coordinates  $(\Delta, \epsilon)$  through a simple translation of the origin:

$$\begin{pmatrix} \Delta' \\ \epsilon' \end{pmatrix} = \begin{pmatrix} \Delta \\ \epsilon \end{pmatrix} + \frac{1}{\sqrt{2}} \begin{pmatrix} -U' \\ U' - U \end{pmatrix}. \quad (22)$$

This gives rise to the Heisenberg exchange for large negative  $\epsilon'$  (from Equation (19)):

$$J(\epsilon') = E_{\text{Triplet}} - E_{\text{Singlet}}^+ \approx \frac{\sqrt{2}t_{12}^2}{|\epsilon'|}, \quad \epsilon' < 0, \quad |\epsilon'| \gg 2t_{12}. \quad (23)$$

By pulsing  $\epsilon' = \epsilon'(t)$ , the exchange  $J(\epsilon'(t))$  can be pulsed on and off again in order to implement the  $\sqrt{\text{SWAP}}$  operation, as described in Section 2 (see the inset of Figure 6). This operation has now been achieved experimentally with a gating time on the order of 180 ps (Petta et al. 2005a), in good agreement with the predictions in (Burkard et al. 1999) for an achievable switching time.

#### 4.4 Initialization of two-spin encoded qubits

Fluctuations in a nuclear spin environment can lead to rapid decoherence of single-electron spin states due to the contact hyperfine interaction (see Section 5, below). The effects of these fluctuations can be reduced, in part, by considering a qubit encoded in two-electron singlet  $|0\rangle = |S(1,1)\rangle$  and triplet states  $|1\rangle = |T_0\rangle$ , as defined in equations (15), (16). With this encoding scheme, the qubit energy splitting would be provided through the exchange coupling (Equation (23)), and single-qubit rotations could be performed using an inhomogeneous magnetic field (Levy 2002). Two-qubit operations in this scheme could be performed, for example, using capacitive coupling due to the relative charge distributions of the triplet and singlet states in neighboring double-dots (Taylor et al. 2005), although the difference in these charge distributions can lead to additional dephasing due to fluctuations in the electrical environment (Coish and Loss 2005) (see also Section 5, below). An alternative scheme to couple such encoded qubits over long distances with optical cavity modes has also been proposed (Burkard and Imamoglu 2006). One additional advantage of the two-spin encoded qubit scheme is that adiabatic tuning of the gate voltages can be used to initialize and readout information stored in the singlet-triplet

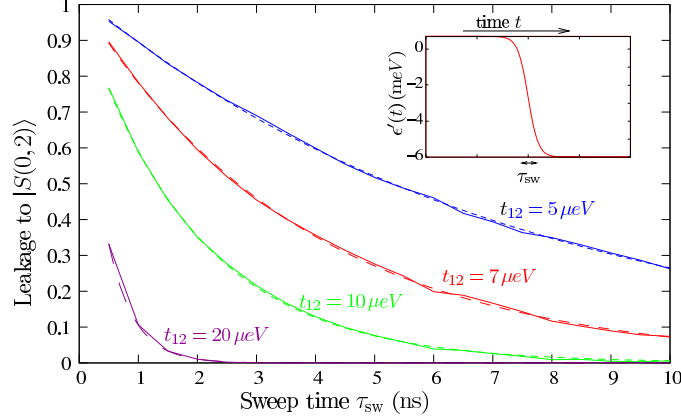


Figure 7: Leakage (the occupation probability of the state  $|S(0, 2)\rangle$ ) at the end of the sweep) due to nonadiabatic transitions after sweeping from  $\epsilon' = 0.7 \text{ meV}$  to  $\epsilon' = -6 \text{ meV}$ . Leakage is given as a function of the characteristic sweep time  $\tau_{\text{sw}}$ , where  $\epsilon'(t) = \epsilon_0 - \frac{\Delta\epsilon}{2} \tanh(2t/\tau_{\text{sw}})$ , with  $\epsilon_0 = -2.65 \text{ meV}$  and  $\Delta\epsilon = 6.7 \text{ meV}$ . We show results for  $t_{12} = 5, 7, 10, 20 \mu\text{eV}$ . Solid lines show the results of numerical integration of the Schrödinger equation and dashed lines give exponential fits, which decay with the time constants  $\tau_{\text{fit}}$ , given in Table 1.

basis (Johnson et al. 2005a, Petta et al. 2005a). We discuss this initialization scheme in the rest of this section.

We consider the singlet ground-state  $|E_{\text{Singlet}}^+\rangle$ , given by Equations (20) and (21). For large positive detuning,  $|\epsilon'| \gg t_{12}, \epsilon' > 0$ , the mixing angle in Equation (21) is  $\theta_+^S \approx \pi$  and the singlet ground state is approximately given by  $|S(0, 2)\rangle$ . For large negative detuning  $|\epsilon'| \gg t_{12}, \epsilon' < 0$ , we find  $\theta_+^S \approx 0$  and the lowest-energy singlet is instead given by  $|S(1, 1)\rangle$  (see Figure 6). If the two-electron system is allowed to relax to its ground state  $|S(0, 2)\rangle$  at large positive detuning  $\epsilon'$  and the detuning is then varied adiabatically slowly to large negative values, the encoded qubit can be initialized to the state  $|0\rangle = |S(1, 1)\rangle$  (see Figure 6 and insets). It is a straightforward exercise to estimate the error in such an operation for a two-dimensional Hamiltonian.

For a linear ramp of  $\epsilon'$  over an infinite interval (i.e.,  $\epsilon' = (\Delta\epsilon/\tau_{\text{sw}})t$ ,  $t = -\infty \dots \infty$  with characteristic switching time  $\tau_{\text{sw}}$  to sweep over an interval  $\Delta\epsilon$ ), the result of Zener, for the non-adiabatic Landau-Zener transition probability is (Zener 1932)

$$P = \exp\left(-\frac{\tau_{\text{sw}}}{\tau_{LZ}}\right), \quad \tau_{LZ} = \frac{\hbar\sqrt{2}\Delta\epsilon}{4\pi t_{12}^2}. \quad (24)$$

Here, the Landau-Zener tunneling probability is controlled in terms of two time scales: the switching time  $\tau_{\text{sw}}$  for a typical range of  $\Delta\epsilon$  and the Landau-Zener time constant  $\tau_{LZ}$ , which has a strong dependence ( $\propto 1/t_{12}^2$ ) on the inter-dot

$t_{12}$ ( $\mu eV$ )	$\tau_{LZ}$ (ns)	$\tau_{\text{fit}}$ (ns)
5	20.	7.4
7	10.	3.8
10	4.9	1.9
20	1.2	0.43

Table 1: Landau-Zener time constant  $\tau_{LZ}$  for a linear ramp of  $\epsilon'$  and the time constant  $\tau_{\text{fit}}$  for fits to numerically evaluated data at various values of the tunnel coupling  $t_{12}$ .

tunnel coupling. For a realistic voltage pulse,  $\epsilon'$  is swept over a finite interval, and the pulse shape, in general, will not be linear for the entire sweep. Performing an analysis similar to that used for single-spin gates (Schliemann et al. 2001, Requist et al. 2005) for this case, one can perform a numerical integration of the time-dependent Schrödinger equation in the subspace formed by the two singlets for an arbitrary pulse shape. We have done this for a pulse of the form  $\epsilon'(t) = \epsilon_0 - \frac{\Delta\epsilon}{2} \tanh(2t/\tau_{\text{sw}})$ ,  $t = -5\tau_{\text{sw}} \dots 5\tau_{\text{sw}}$ <sup>1</sup>, where we find an approximately exponential dependence of  $P$  on the switching time  $\tau_{\text{sw}}$  (see Figure 7). Fitting to this exponential dependence, we find a time constant  $\tau_{\text{fit}}$  analogous to the Landau-Zener time  $\tau_{LZ}$ . The time constants  $\tau_{LZ}$  (from Equation (24)) and  $\tau_{\text{fit}}$  from the numerical data in Figure 7 are compared in Table 1 for various values of the inter-dot tunnel coupling  $t_{12}$ . The results of Figure 7 and Table 1 suggest that (for this set of parameters) adiabatic switching for initialization or readout on a time scale of  $\tau_{\text{sw}} \lesssim 1$  ns can only be performed without significant error if the tunnel coupling  $t_{12}$  is made larger than  $t_{12} > 20 \mu eV$ . It is important to note that this analysis ignores additional effects due to magnetic field inhomogeneities, spin-orbit coupling, or the hyperfine interaction, all of which can lead to additional singlet-triplet anticrossings (see Section 5.2, below) and hence, to additional initialization or readout errors.

## 5 DECOHERENCE

Decoherence is the process by which information stored in a quantum bit is lost. There are two time scales used to describe decoherence processes for a spin that decays exponentially in the presence of an applied magnetic field.  $T_1$  is the longitudinal spin decay time, or spin-flip time, which describes the time scale for random spin flips:  $|\uparrow\rangle \rightarrow |\downarrow\rangle$ .  $T_2$ , the transverse spin decay time, describes the decay of a superposition state  $a|\uparrow\rangle + b|\downarrow\rangle$ . Both of these time scales are important for quantum computing, since both effects lead to qubit errors.

An experiment performed on an ensemble of systems with different environ-

<sup>1</sup>Note that this type of pulse will generally lead to a smaller value of  $P$  for a given set of parameters since here,  $d\epsilon'/dt \leq \Delta\epsilon/\tau_{\text{sw}}$ , whereas for the linear pulse  $d\epsilon'/dt = \Delta\epsilon/\tau_{\text{sw}}$  for the entire sweep.

ments can lead to additional decoherence, beyond that described by the “intrinsic”  $T_2$  time (Slichter 1980). For such an experiment, the ensemble-averaged transverse spin decay time is therefore often denoted  $T_2^*$  to distinguish it from the single-spin decay time. Other symbols such as  $\tau_c$  (the correlation time) and  $T_M$  (the magnetization envelope decay time) are often used to distinguish decay that is non-exponential.

For a quantum-dot-confined electron spin state to decay, it is necessary for the spin to couple in some way to fluctuations in the environment. There are two important sources of this coupling for electron spins in quantum dots. First, the spin-orbit interaction couples electron spin states to their orbital states, and therefore makes spins indirectly sensitive to fluctuations in the electric environment. Second, the Fermi contact hyperfine interaction between electrons and surrounding nuclear spins in the host material can lead to rapid decay if fluctuations in the nuclear spin environment are not properly controlled. In the rest of this section we discuss recent progress in understanding decoherence due to these two coupling mechanisms.

## 5.1 Spin-orbit interaction

For a 2DEG formed in GaAs, the spin-orbit interaction is given in terms of two terms:

$$H_{\text{SO}} = \alpha (p_x \sigma_y - p_y \sigma_x) + \beta (p_y \sigma_y - p_x \sigma_x) + O(|\mathbf{p}|^3), \quad (25)$$

where  $\sigma_{x,y}$  are Pauli matrices and  $\mathbf{p} = (p_x, p_y)$  is the momentum operator in the plane of the 2DEG. The first term, proportional to  $\alpha$ , is the Rashba (or structure-inversion-asymmetry) spin-orbit coupling term. The Rashba term is due to asymmetry in the confining potential and can therefore be tuned to some degree with applied gates. The second term, proportional to  $\beta$ , is the Dresselhaus (bulk-inversion-asymmetry) term, and is due to the fact that GaAs, which has a zincblende lattice, has no center of inversion symmetry. Corrections to this spin-orbit Hamiltonian of order  $|\mathbf{p}|^3$  are smaller than the linear-momentum terms in quantum dots by the ratio of  $z$ -confinement length to the quantum-dot Bohr radius, and are negligible in the two-dimensional limit (Cerletti et al. 2005).

$H_{\text{SO}}$  obeys time-reversal symmetry. Thus, in the absence of a magnetic field, the ground state of a single electron confined to a quantum dot is twofold degenerate due to Kramer’s theorem, and  $H_{\text{SO}}$  alone can not cause decoherence. The character of the ground-state doublet does change, however, due to the presence of  $H_{\text{SO}}$ , mixing orbital and spin states. Thus, any fluctuations that couple to the orbital degree of freedom can cause decoherence in combination with spin-orbit coupling. These fluctuations can come from lattice phonons, surrounding gates, electron-hole pair excitations, etc. (Golovach et al. 2004). The longitudinal-spin relaxation rate  $1/T_1$  due to spin-orbit coupling and lattice phonons has been calculated, and shows a strong suppression for confined electrons (with large level spacing  $\hbar\omega_0$ ) in weak magnetic fields:  $1/T_1 \propto B^5 / (\hbar\omega_0)^4$  (Khaetskii and Nazarov 2000, Khaetskii and Nazarov 2001). This calculation

has been extended to a larger range of magnetic fields, showing that the  $B$ -field dependence of  $1/T_1$  saturates and is then suppressed when the phonon wavelength is comparable to the dot size (Golovach et al. 2004). Further, this calculation has also been extended to include the transverse spin decay time due to spin-orbit interaction alone, showing that dephasing is limited by relaxation, or  $T_2 = 2T_1$  to leading order in the spin-orbit coupling, independent of the particular source of fluctuations (Golovach et al. 2004). Additionally,  $1/T_1$  has been shown to have a strong dependence on the magnetic field direction, relative to the crystal axes (Fal'ko et al. 2005), shows a strong enhancement near avoided level crossings, which may allow independent measurements of the Rashba and Dresselhaus coupling constants (Bulaev and Loss 2005*a*), and plays a role in phonon-assisted cotunneling current through quantum dots (Lehmann and Loss 2006). The relaxation rate of quantum-dot-confined hole spins due to spin-orbit coupling and phonons has also been investigated. In some cases, recent work has shown that the hole spin relaxation time may even exceed the relaxation time of electron spins (Bulaev and Loss 2005*b*). In addition to lattice phonons, electric field fluctuations can result from the noise in a QPC readout device, which results in spin decoherence when considered in combination with spin-orbit coupling. This mechanism shows a strong dependence of the decoherence rate  $\sim 1/r^6$  on the dot-QPC separation  $r$  (Borhani et al. 2005), and can therefore be controlled with careful positioning of the readout device.

Measurements of relaxation times for single electron spins have been performed in gated lateral quantum dots (Hanson et al. 2003, Elzerman et al. 2004), giving a  $T_1$  time in good agreement with the theory of ref. (Golovach et al. 2004) and in self-assembled quantum dots (Kroutvar et al. 2004), which confirmed the expected magnetic field dependence:  $1/T_1 \propto B^5$  (Khaetskii and Nazarov 2001). Additionally, singlet-triplet decay has been measured in single vertical (Fujisawa et al. 2002), and lateral (Hanson et al. 2005) dots, as well as lateral double dots (Petta et al. 2005*b*, Johnson et al. 2005*a*).

There is a general consensus that spin relaxation for quantum-dot-confined electrons proceeds through the spin-orbit interaction and phonon emission at high magnetic fields. However, in weak magnetic fields, and for the transverse spin decay time  $T_2$ , there are stronger effects in GaAs. These effects are due to the contact hyperfine interaction between confined electron spins and nuclear spins in the surrounding lattice.

## 5.2 Hyperfine interaction

For a collection of electrons in the presence of nuclear spins, the Fermi contact hyperfine interaction reads

$$H_{\text{hf}} = Av \sum_k \mathbf{I}_k \cdot \mathbf{S}(\mathbf{r}_k), \quad \mathbf{S}(\mathbf{r}_k) = \frac{1}{2} \sum_{\sigma, \sigma'=\uparrow, \downarrow} \psi_{\sigma}^{\dagger}(\mathbf{r}_k) \boldsymbol{\sigma}_{\sigma\sigma'} \psi_{\sigma'}(\mathbf{r}_k), \quad (26)$$

where  $A$  is the hyperfine coupling strength,  $v$  is the volume of a crystal unit cell containing one nuclear spin,  $\mathbf{I}_k$  is the spin operator for the nuclear spin at site

$k$ ,  $\mathbf{S}(\mathbf{r}_k)$  is the electron spin density at the nuclear site, given in terms of field operators  $\psi_\sigma(\mathbf{r})$  that satisfy the anticommutation relations  $\{\psi_\sigma(\mathbf{r}), \psi_{\sigma'}^\dagger(\mathbf{r}')\} = \delta(\mathbf{r} - \mathbf{r}')\delta_{\sigma,\sigma'}$ ,  $\{\psi_\sigma(\mathbf{r}), \psi_{\sigma'}(\mathbf{r}')\} = 0$ , and we have denoted matrix elements by  $\sigma_{\sigma\sigma'} = \langle \sigma | \boldsymbol{\sigma} | \sigma' \rangle$ , where  $\boldsymbol{\sigma} = (\sigma_x, \sigma_y, \sigma_z)$  is the vector of Pauli matrices. The significance of the general form given in Equation (26) is that there can be an interplay of orbital and spin degrees of freedom due to the contact hyperfine interaction. When the orbital level spacing is not too large, this interplay can be the limiting cause of electron-spin relaxation (Erlingsson et al. 2001, Erlingsson and Nazarov 2002) in weak magnetic fields, where the spin-orbit interaction is less effective, and leads to enhanced nuclear spin relaxation in the vicinity of sequential-tunneling peaks for a quantum dot connected to leads, where  $\mathbf{S}(\mathbf{r})$  fluctuates significantly (Lyanda-Geller et al. 2002, Hüttel et al. 2004).

The orbital level spacing in lateral quantum dots is usually much larger than the typical energy scale of  $H_{\text{hf}}$ . In this case, it is possible to solve for the orbital envelope wavefunction  $\Psi_0(\mathbf{r})$  in the absence of the hyperfine interaction, and write an effective hyperfine Hamiltonian for a single electron confined to the quantum-dot orbital ground state:

$$H_{\text{hf},0} \approx \mathbf{h}_0 \cdot \mathbf{S}_0, \quad \mathbf{h}_0 = Av \sum |\Psi_0(\mathbf{r}_k)|^2 \mathbf{I}_k, \quad (27)$$

where here  $\mathbf{S}_0$  is the spin-1/2 operator for a single electron in the quantum-dot orbital ground state. The primary material used to make lateral quantum dots is GaAs. All natural isotopes of Ga and As carry nuclear spin  $I = 3/2$ . Each isotope has a distinct hyperfine coupling constant, but the average coupling constant, weighted by the relative abundance of each isotope in GaAs gives  $A \approx 90 \mu\text{eV}$  (Paget et al. 1977).

Dynamics under  $H_{\text{hf},0}$  have now been studied extensively under many various approximations and in many parameter regimes. Here we give a brief account of some part of this study. For an extensive overview, see reviews in (Schliemann et al. 2003, Cerletti et al. 2005). The first analysis of the influence of Equation (27) on quantum-dot electron spin dynamics showed that the long-time longitudinal spin-flip probability,  $P_{\uparrow\downarrow} \approx 1/p^2 N$  (Burkard et al. 1999) was suppressed in the limit of large nuclear spin polarization  $p$  and number of nuclear spins in the dot,  $N$ . Subsequently, an exact solution for the case of a fully-polarized nuclear spin system ( $p = 1$ ) has shown that both the longitudinal and transverse components of the electron spin decay by a fraction  $\sim 1/N$  according to a long-time power law  $\sim 1/t^{3/2}$  on a time scale of  $\tau \sim \hbar N/A$  (Khaetskii et al. 2002) ( $\hbar N/A \sim 1 \mu\text{s}$  for a GaAs dot containing  $N \simeq 10^5$  nuclei). This exact solution for  $p = 1$ , which shows a non-exponential decay, demonstrates that the electron spin decay is manifestly non-Markovian since the time scale for motion in the nuclear-spin bath is much longer than the decay time scale of the electron spin. For unpolarized systems, the ensemble averaged mean-field dynamics show a transverse spin decay on a time scale  $\tau \sim \hbar\sqrt{N}/A \sim 5 \text{ ns}$  (Khaetskii et al. 2002, Merkulov et al. 2002). The exact solution has been extended to the case of nonzero polarization  $p \neq 1$  using a generalized master equation, valid in the limit of large magnetic field or polarization  $p \gg 1/\sqrt{N}$

(Coish and Loss 2004). This work has shown that, while the longitudinal spin decay is bounded by  $\sim 1/p^2 N$ , due to the quantum nature of the nuclear field, the transverse components of spin will decay to zero in a time  $t_c \approx 5 \text{ ns}/\sqrt{1-p^2}$  (without ensemble averaging and without making a mean-field ansatz), unless an electron spin echo sequence is performed or the nuclei are prepared in an eigenstate of the operator  $h_0^z$  through measurement (Coish and Loss 2004). There are several recent suggestions for methods that could be used to measure the operator  $h_0^z$  (Giedke et al. 2005, Klauser et al. 2005, Stepanenko et al. 2005) in order to extend electron spin decoherence. Once the nuclear spin system is forced into an eigenstate of  $h_0^z$ , the lowest-order corrections for large magnetic field still show incomplete decay for the transverse spin (Coish and Loss 2004), suggesting that dynamics induced by the nuclear dipolar interaction may limit spin coherence in this regime (de Sousa and Das Sarma 2003), although higher-order corrections have been reported to lead to complete decay (Deng and Hu 2005), even when the nuclear spin system is static. There have been several efforts to understand the hyperfine decoherence problem numerically (Schliemann et al. 2002, Shenvi et al. 2005b), and other studies have investigated electron spin-echo envelope decoherence under the hyperfine interaction alone (Coish and Loss 2004, Shenvi et al. 2005b, Shenvi et al. 2005a) or the combined influence of hyperfine and nuclear dipolar interactions (de Sousa and Das Sarma 2003, de Sousa et al. 2005, Witzel et al. 2005, Yao et al. 2005, Yao et al. 2006). Other approaches to understanding the hyperfine decoherence problem include semi-classical theories that replace the quantum nuclear field by a classical dynamical vector (Erlingsson and Nazarov 2004, Yuzbashyan et al. 2004) or a classical distribution function (Al-Hassanieh et al. 2005).

Experiments on electron spin decoherence in single quantum dots (Bracker et al. 2005, Dutt et al. 2005) and double quantum dots (Petta et al. 2005a, Koppens et al. 2005) have now confirmed that the ensemble-averaged electron spin dephasing time is indeed given by  $\tau \sim \hbar\sqrt{N}/A \sim 10 \text{ ns}$ .

For two electron spins confined to a double quantum dot, the hyperfine Hamiltonian (Equation (26)) can be cast in the form (Coish and Loss 2005)

$$H_{\text{hf,dd}} = \epsilon_z S_l^z + \sum_l \mathbf{h}_l \cdot \mathbf{S}_l; \quad \mathbf{S}_l = \frac{1}{2} \sum_{\sigma, \sigma'=\uparrow, \downarrow} d_{l\sigma}^\dagger \boldsymbol{\sigma}_{\sigma\sigma'} d_{l\sigma'}, \quad (28)$$

$$= \epsilon_z S_l^z + \mathbf{S} \cdot \mathbf{h} + \delta \mathbf{S} \cdot \delta \mathbf{h}, \quad (29)$$

where  $\epsilon_z = g\mu_B B$  is the Zeeman splitting,  $d_{1(2)\sigma}$  annihilates an electron in the single-particle orbital state with envelope wavefunction  $\Psi_{1(2)}(\mathbf{r})$  and spin  $\sigma$ , we define  $\mathbf{h} = (\mathbf{h}_1 + \mathbf{h}_2)/2$ ,  $\delta \mathbf{h} = (\mathbf{h}_1 - \mathbf{h}_2)/2$ , where the quantum nuclear field operators are  $\mathbf{h}_{1(2)} = Av \sum_k |\Psi_{1(2)}(\mathbf{r}_k)|^2 \mathbf{I}_k$ , the sum of electron spins is  $\mathbf{S} = \mathbf{S}_1 + \mathbf{S}_2$  and the difference is  $\delta \mathbf{S} = \mathbf{S}_1 - \mathbf{S}_2$ . While the sum  $\mathbf{S}$  conserves the total squared electron spin, and can only couple states of different  $z$ -projection (e.g.  $|T_0\rangle$  to  $|T_\pm\rangle$ ), the difference  $\delta \mathbf{S}$  does not preserve the total spin, and therefore couples singlet to triplet (e.g.  $|S(1,1)\rangle$  to  $|T_0\rangle$  and  $|T_\pm\rangle$ ) and will therefore lead to anticrossings in the energy level spectrum, where  $|S(1,1)\rangle$  and  $|T_\pm\rangle$

or  $|T_0\rangle$  cross. Adding Equation (29) to the previous double-dot hamiltonian,  $H_{\text{dd}} = H_{\text{C}} + H_{\text{T}} + H_{\text{hf,dd}}$ , and making a mean-field ansatz for the nuclear field operators, i.e., replacing operators by their expectation values:  $\mathbf{h} \rightarrow \langle \mathbf{h} \rangle$ ,<sup>2</sup> leads to the energy level spectrum shown in Figure 6. In the limit of large Zeeman splitting  $\epsilon_z$  and large negative detuning  $\epsilon'$ , an effective two-level Hamiltonian can be derived in the subspace of lowest-energy singlet and  $S^z = 0$  triplet ( $|S\rangle, |T_0\rangle$ ) (Coish and Loss 2005):

$$H_{\text{dd,eff}} = \frac{J}{2} \mathbf{S} \cdot \mathbf{S} + \delta h^z \delta S^z + O\left(\frac{1}{\epsilon_z}\right). \quad (30)$$

An exact solution can be found for pseudospin dynamics in the two-dimensional subspace of  $|S\rangle$  and  $|T_0\rangle$  under the action of  $H_{\text{dd,eff}}$ . This solution shows that a singlet-triplet correlator undergoes an interesting power-law decay in a characteristic time scale that can be extended by increasing  $J$  (Coish and Loss 2005), and has been verified in experiment (Laird et al. 2005). As is true for the transverse components of a single electron spin, the singlet-triplet correlator shows a rapid decay if the nuclear spin environment is not in an eigenstate of the relevant nuclear field operator (in this case,  $\delta h^z$ ). The decay time can be significantly extended by narrowing the distribution in  $\delta h^z$  eigenstates through measurement (Klauser et al. 2005) or by performing a spin-echo sequence (Petta et al. 2005a). Remaining sources of dephasing include the corrections to  $H_{\text{dd,eff}}$  (of order  $1/\epsilon_z$ , which can not be removed easily) and fluctuations in the electrostatic environment, although the effect of these fluctuations can be removed to leading order at zero-derivative points for the exchange interaction (Coish and Loss 2005), where:

$$\frac{dJ(\epsilon)}{d\epsilon} = 0. \quad (31)$$

Recent calculations suggest that these zero-derivative points should be achievable with appropriate control of the confinement potential or magnetic field (Hu and Das Sarma 2006, Stopa and Marcus 2006).

Since the hyperfine interaction does not preserve the total spin quantum number of electrons, this interaction plays a very important role in studies on spin-dependent transport. In particular, spin blockade (Weinmann et al. 1995, Weinmann 2003) occurs in double quantum dots (Ono et al. 2002) when tunneling is allowed between spin-singlets  $|S(1,1)\rangle \rightarrow |S(0,2)\rangle$ , but not between spin triplets  $|T(1,1)\rangle \leftrightarrow |T(0,2)\rangle$ , because of a large energy cost due to orbital level spacing and the Pauli principle. This blockade allows for the extraction of features at energy scales much less than temperature, making it an ideal parameter regime in which to perform spectroscopy on double dots (Pioro-Ladrière et al. 2003) and spin-resonance experiments, which previously suffered from “heating” effects in single dots (van der Wiel et al. 2003, Koppens et al. 2006). The hyperfine interaction mixes the  $|S(1,1)\rangle$  and  $|T(1,1)\rangle$  states, allowing transport, and effectively removing spin blockade when these states are nearly degenerate. This behavior leads to a number of intriguing effects, including stable

<sup>2</sup>In general, great care should be taken in making such a replacement. See the discussion, for example, in (Coish and Loss 2005).



undriven oscillations in transport current (Ono and Tarucha 2004, Erlingsson et al. 2005), and a striking magnetic-field dependence of leakage current, which allows the extraction of information about the nuclear spin system (Koppens et al. 2005, Jouravlev and Nazarov 2006). Even-odd effects in the spin blockade of many-electron quantum dots have further revealed the shell-filling illustrated in Figure 3 (Johnson et al. 2005*b*).

The influence of spin-dependent terms, causing decoherence or unwanted evolution, is a central issue in quantum-dot spin quantum computing. The requirements for fault-tolerant quantum information processing are very stringent. This raises the bar for required understanding of these environmental influences to a very high level, and guarantees that quantum-dot spin decoherence will remain a challenge for some time to come.

## 6 ENTANGLEMENT GENERATION, DISTILLATION, AND DETECTION

In addition to the usual requirements for control and coherence, to demonstrate the true quantum nature of qubits, there have been many suggestions to create and measure nonlocal multiparticle entanglement of electron spins in nanostructures (DiVincenzo and Loss 1999, Burkard et al. 2000, Loss and Sukhorukov 2000, Choi et al. 2000, Egues et al. 2002, Burkard and Loss 2003, Samuelsson et al. 2004, Recher et al. 2001, Lesovik et al. 2001, Mélin 2001, Costa and Bose 2001, Oliver et al. 2002, Bose and Home 2002, Recher and Loss 2002, Bena et al. 2002, Saraga and Loss 2003, Bouchiat et al. 2003, Recher and Loss 2003, Beenakker and Schoenenberger 2003, Saraga et al. 2004, Egues et al. 2005). These proposals include suggestions to extract spin singlets from a superconductor through two quantum dots (Recher et al. 2001) or nanotubes (Recher and Loss 2002, Bena et al. 2002), or to create entanglement near a magnetic impurity (Costa and Bose 2001), through a single quantum dot (Oliver et al. 2002), from biexcitons in double quantum dots (Gywat et al. 2002), or through a triple dot (Saraga and Loss 2003). It may also be possible to distill entanglement (Bennett et al. 1997) from an unentangled Fermi gas through Coulomb scattering in a 2DEG (Saraga et al. 2004).

As well as providing a proof of quantum mechanical behavior, entanglement can be used as a resource for measurement-based quantum computing. Some measurement-based schemes rely on the creation of highly-entangled cluster states (Raussendorf and Briegel 2001), which could be generated in quantum-dot arrays using the Heisenberg exchange interaction (Borhani and Loss 2005). Other measurement-based schemes generate entanglement through partial Bell-state (parity) measurements (Beenakker et al. 2004), which could also be implemented for spins in quantum dots using spin-to-charge conversion (Engel and Loss 2005). Independent of the method used, the generation or purification and subsequent detection of entangled electron spins would present a significant milestone on the road to a working quantum-dot quantum computer.

## 7 CONCLUSIONS AND OUTLOOK

We have presented some of the theoretical and experimental challenges to quantum-dot quantum computing with electron spins. The last few years have seen an extremely rapid rate of progress in experiments which show that many of the required elements of a spin-based quantum-dot quantum computer can be realized in principle. The most significant advances include the reduction of the number of electrons confined to gated quantum dots down to a single electron (Ciorga et al. 2000), the demonstration (Hanson et al. 2003) and improvement (Hanson et al. 2005) of electron spin readout in gated lateral dots, which has led to the measurement of a spin  $T_1$  time (Elzerman et al. 2004), the demonstration of the  $\sqrt{\text{SWAP}}$  operation, allowing for the extraction of an ensemble-averaged  $T_2^*$  time, and spin-echo methods to extend the decay time within a two-spin encoded subspace (Petta et al. 2005a), and most recently the demonstration of single-spin rotations under resonant conditions (Koppens et al. 2006).

To demonstrate viability of the Loss-DiVincenzo proposal, more experiments are needed. Although the Loss-DiVincenzo proposal is scalable in principle, it remains to be seen if there are significant practical obstacles to scaling-up the number of electrons involved well beyond two.

**Acknowledgments:** We acknowledge financial support from the Swiss NSF, the NCCR Nanoscience, EU NoE MAGMANet, DARPA, ARO, ONR, and JST ICORP.

## References

- Al-Hassanieh, K. A., Dobrovitski, V. V., Dagotto, E. and Harmon, B. N. (2005). Numerical modeling of the central spin problem using the spin coherent states p-representation. <http://arXiv.org/cond-mat/0511681>.
- Atature, M., Dreiser, J., Badolato, A., Hogele, A., Karrai, K. and Imamoglu, A. (2006). Quantum-Dot Spin-State Preparation with Near-Unity Fidelity. *Science*, **312**, 551–553.
- Awschalom, D. D., Loss, D. and Samarth, N. (2002). *Semiconductor Spintronics and Quantum Computing*. Springer-Verlag, Berlin.
- Badolato, A., Hennessy, K., Atature, M., Dreiser, J., Hu, E., Petroff, P. M. and Imamoglu, A. (2005). Deterministic Coupling of Single Quantum Dots to Single Nanocavity Modes. *Science*, **308**, 1158–1161.
- Barenco, A., Bennett, C. H., Cleve, R., DiVincenzo, D. P., Margolus, N., Shor, P., Sleator, T., Smolin, J. A. and Weinfurter, H. (1995). Elementary gates for quantum computation. *Phys. Rev. A*, **52**, 3457–3467.
- Barenco, A., Deutsch, D., Ekert, A. and Jozsa, R. (1995). Conditional Quantum Dynamics and Logic Gates. *Phys. Rev. Lett.*, **74**, 4083–4086.

- Bayer, M., Hawrylak, P., Hinzer, K., Fafard, S., Korkusinski, M., Wasilewski, Z. R., Stern, O. and Forchel, A. (2001). Coupling and Entangling of Quantum States in Quantum Dot Molecules. *Science*, **291**, 451–453.
- Beenakker, C. W., DiVincenzo, D. P., Emary, C. and Kindermann, M. (2004). Charge Detection Enables Free-Electron Quantum Computation. *Phys. Rev. Lett.*, **93**, 020501.
- Beenakker, C. W. J. (1991). Theory of Coulomb-blockade oscillations in the conductance of a quantum dot. *Phys. Rev. B*, **44**, 1646–1656.
- Beenakker, C. W. J. and Schoenenberger, C. (2003). Quantum shot noise. *Physics Today*, May 2003p. 37.
- Bena, C., Vishveshwara, S., Balents, L. and Fisher, M. P. (2002). Quantum Entanglement in Carbon Nanotubes. *Phys. Rev. Lett.*, **89**, 037901.
- Bennett, C. H., Brassard, G., Popescu, S., Schumacher, B., Smolin, J. A. and Wootters, W. K. (1997). Purification of Noisy Entanglement and Faithful Teleportation via Noisy Channels. *Phys. Rev. Lett.*, **78**, 2031.
- Biercuk, M., Garaj, S., Mason, N., Chow, J. and Marcus, C. (2005). Gate-defined quantum dots on carbon nanotubes. *Nano Letters*, **5**, 1267–1271.
- Blick, R. H., Pfannkuche, D., Haug, R. J., Klitzing, K. V. and Eberl, K. (1998). Formation of a Coherent Mode in a Double Quantum Dot. *Phys. Rev. Lett.*, **80**, 4032–4035.
- Bonesteel, N. E., Stepanenko, D. and DiVincenzo, D. P. (2001). Anisotropic Spin Exchange in Pulsed Quantum Gates. *Phys. Rev. Lett.*, **87**, 207901.
- Borhani, M. and Loss, D. (2005). Cluster states from Heisenberg interactions. *Phys. Rev. A*, **71**, 034308.
- Borhani, M., Golovach, V. N. and Loss, D. (2005). Spin decay in a quantum dot coupled to a quantum point contact. <http://arXiv.org/cond-mat/0510758>.
- Bose, S. and Home, D. (2002). Generic Entanglement Generation, Quantum Statistics, and Complementarity. *Phys. Rev. Lett.*, **88**, 050401.
- Bouchiat, V., Chtchelkatchev, N., Feinberg, D., Lesovik, G. B., Martin, T. and Torrès, J. (2003). Single-walled carbon nanotube superconductor entangler: noise correlations and Einstein Podolsky Rosen states. *Nanotechnology*, **14**, 77–85.
- Bracker, A. S., Stinaff, E. A., Gammon, D., Ware, M. E., Tischler, J. G., Shabaev, A., Efros, A. L., Park, D., Gershoni, D., Korenev, V. L. and Merkulov, I. A. (2005). Optical Pumping of the Electronic and Nuclear Spin of Single Charge-Tunable Quantum Dots. *Phys. Rev. Lett.*, **94**, 047402.

- Brodsky, M., Zhitenev, N. B., Ashoori, R. C., Pfeiffer, L. N. and West, K. W. (2000). Localization in Artificial Disorder: Two Coupled Quantum Dots. *Physical Review Letters*, **85**, 2356–2359.
- Bulaev, D. V. and Loss, D. (2005a). Spin relaxation and anticrossing in quantum dots: Rashba versus Dresselhaus spin-orbit coupling. *Phys. Rev. B*, **71**, 205324.
- Bulaev, D. V. and Loss, D. (2005b). Spin Relaxation and Decoherence of Holes in Quantum Dots. *Phys. Rev. Lett.*, **95**, 076805.
- Burkard, G. (2004). Theory of solid state quantum information processing. <http://arXiv.org/cond-mat/0409626>.
- Burkard, G. and Imamoglu, A. (2006). Ultra-long distance interaction between spin qubits. <http://arXiv.org/cond-mat/0603119>.
- Burkard, G. and Loss, D. (2002). Cancellation of Spin-Orbit Effects in Quantum Gates Based on the Exchange Coupling in Quantum Dots. *Phys. Rev. Lett.*, **88**, 047903.
- Burkard, G. and Loss, D. (2003). Lower Bound for Electron Spin Entanglement from Beam Splitter Current Correlations. *Phys. Rev. Lett.*, **91**, 087903.
- Burkard, G., Loss, D. and DiVincenzo, D. P. (1999). Coupled quantum dots as quantum gates. *Phys. Rev. B*, **59**, 2070–2078.
- Burkard, G., Loss, D. and Sukhorukov, E. V. (2000). Noise of entangled electrons: Bunching and antibunching. *Phys. Rev. B*, **61**, 16303.
- Cerletti, V., Coish, W. A., Gywat, O. and Loss, D. (2005). Recipes for spin-based quantum computing. *Nanotechnology*, **16**, R27.
- Choi, M.-S., Bruder, C. and Loss, D. (2000). Spin-dependent Josephson current through double quantum dots and measurement of entangled electron states. *Phys. Rev. B*, **62**, 13569–13572.
- Chutia, S., Friesen, M. and Joynt, R. (2006). Detection and measurement of the dzyaloshinskii-moriya interaction in double quantum dot systems.
- Ciorga, M., Sachrajda, A. S., Hawrylak, P., Gould, C., Zawadzki, P., Jullian, S., Feng, Y. and Wasilewski, Z. (2000). Addition spectrum of a lateral dot from Coulomb and spin-blockade spectroscopy. *Phys. Rev. B*, **61**, 16315.
- Cirac, J. I. and Zoller, P. (1995). Quantum Computations with Cold Trapped Ions. *Phys. Rev. Lett.*, **74**, 4091–4094.
- Coish, W. A. and Loss, D. (2004). Hyperfine interaction in a quantum dot: Non-markovian electron spin dynamics. *Phys. Rev. B*, **70**, 195340.

- Coish, W. A. and Loss, D. (2005). Singlet-triplet decoherence due to nuclear spins in a double quantum dot. *Phys. Rev. B*, **72**, 125337.
- Cortez, S., Krebs, O., Laurent, S., Senes, M., Marie, X., Voisin, P., Ferreira, R., Bastard, G., Gerard, J.-M. and Amand, T. (2002). Optically driven spin memory in *n*-doped InAs-GaAs quantum dots. *Phys. Rev. Lett.*, **89**, 207401.
- Costa, A. T. and Bose, S. (2001). Impurity Scattering Induced Entanglement of Ballistic Electrons. *Phys. Rev. Lett.*, **87**, 277901.
- de Sousa, R. and Das Sarma, S. (2003). Electron spin coherence in semiconductors: Considerations for a spin-based solid-state quantum computer architecture. *Phys. Rev. B*, **67**, 033301.
- de Sousa, R., Shenvi, N. and Whaley, K. B. (2005). Qubit coherence control in a nuclear spin bath. *Phys. Rev. B*, **72**, 045330.
- Deng, C. and Hu, X. (2005). Analytical solution of electron spin decoherence through hyperfine interaction in a quantum dot. <http://www.arXiv.org/cond-mat/0510379>.
- DiVincenzo, D. P. (1999). Quantum computing and single-qubit measurements using the spin-filter effect. *Jour. Appl. Phys.*, **85**, 4785–4787.
- DiVincenzo, D. P. (2000). The physical implementation of quantum computation. *Fortschr. Phys.*, **48**, 771.
- DiVincenzo, D. P. and Loss, D. (1999). Quantum computers and quantum coherence. *Journal of Magnetism and Magnetic Materials*, **200**, 202–218.
- Domokos, P., Raimond, J. M., Brune, M. and Haroche, S. (1995). Simple cavity-QED two-bit universal quantum logic gate: The principle and expected performances. *Phys. Rev. A*, **52**, 3554–3559.
- Duckheim, M. and Loss, D. (2006). Electric-dipole-induced spin resonance in disordered semiconductors. *Nat Phys*, **2**, 195–199.
- Dutt, M. V., Cheng, J., Li, B., Xu, X., Li, X., Berman, P. R., Steel, D. G., Bracker, A. S., Gammon, D., Economou, S. E., Liu, R.-B. and Sham, L. J. (2005). Stimulated and Spontaneous Optical Generation of Electron Spin Coherence in Charged GaAs Quantum Dots. *Phys. Rev. Lett.*, **94**, 227403.
- Egues, J. C., Burkard, G. and Loss, D. (2002). Rashba Spin-Orbit Interaction and Shot Noise for Spin-Polarized and Entangled Electrons. *Phys. Rev. Lett.*, **89**, 176401.
- Egues, J. C., Burkard, G., Saraga, D. S., Schliemann, J. and Loss, D. (2005). Shot noise and spin-orbit coherent control of entangled and spin-polarized electrons. *Phys. Rev. B*, **72**, 235326.

- Elzerman, J. M., Hanson, R., Greidanus, J. S., Willems van Beveren, L. H., de Franceschi, S., Vandersypen, L. M., Tarucha, S. and Kouwenhoven, L. P. (2003). Few-electron quantum dot circuit with integrated charge read out. *Phys. Rev. B*, **67**, 161308.
- Elzerman, J. M., Hanson, R., Willems van Beveren, L. H., Witkamp, B., Vandersypen, L. M. K. and Kouwenhoven, L. P. (2004). Single-shot read-out of an individual electron spin in a quantum dot. *Nature*, **430**, 431–435.
- Engel, H.-A. and Loss, D. (2001). Detection of single spin decoherence in a quantum dot via charge currents. *Phys. Rev. Lett.*, **86**, 4648.
- Engel, H.-A. and Loss, D. (2005). Fermionic Bell-State Analyzer for Spin Qubits. *Science*, **309**, 586–588.
- Engel, H.-A., Golovach, V. N., Loss, D., Vandersypen, L. M. K., Elzermann, J. M., Hanson, R. and Kouwenhoven, L. P. (2004). Measurement efficiency and n-shot read out of spin qubits. *Phys. Rev. Lett.*, **93**, 106804.
- Engel, H.-A., Kouwenhoven, L. P., Loss, D. and Marcus, C. M. (2004). Controlling spin qubits in quantum dots. *Quantum Information Processing*, **3**, 115–132.
- Erlingsson, S. I. and Nazarov, Y. V. (2002). Hyperfine-mediated transitions between a Zeeman split doublet in GaAs quantum dots: The role of the internal field. *Phys. Rev. B*, **66**, 155327.
- Erlingsson, S. I. and Nazarov, Y. V. (2004). Evolution of localized electron spin in a nuclear spin environment. *Phys. Rev. B*, **70**, 205327.
- Erlingsson, S. I., Jouravlev, O. N. and Nazarov, Y. V. (2005). Coherent oscillations of current due to nuclear spins. *Phys. Rev. B*, **72**, 033301.
- Erlingsson, S. I., Nazarov, Y. V. and Fal’ko, V. I. (2001). Nucleus-mediated spin-flip transitions in GaAs quantum dots. *Phys. Rev. B*, **64**, 195306.
- Fal’ko, V. I., Altshuler, B. L. and Tsyplatyev, O. (2005). Anisotropy of spin splitting and spin relaxation in lateral quantum dots. *Phys. Rev. Lett.*, **95**, 076603.
- Farhi, E., Goldstone, J., Gutmann, S. and Sipser, M. (2000). Quantum Computation by Adiabatic Evolution. <http://arXiv.org/quant-ph/0001106>.
- Farhi, E., Goldstone, J., Gutmann, S., Lapan, J., Lundgren, A. and Preda, D. (2001). A Quantum Adiabatic Evolution Algorithm Applied to Random Instances of an NP-Complete Problem. *Science*, **292**, 472.
- Fasth, C., Fuhrer, A., Bjork, M. and Samuelson, L. (2005). Tunable double quantum dots in InAs nanowires defined by local gate electrodes. *Nano Letters*, **5**, 1487–1490.

- Fiederling, R., Keim, M., Reuscher, G., Ossau, W., Schmidt, G., Waag, A. and Molenkamp, L. W. (1999). Injection and detection of a spin-polarized current in a light-emitting diode. *Nature*, **402**, 787–790.
- Folk, J. A., Potok, R. M., Marcus, C. M. and Umansky, V. (2003). A Gate-Controlled Bidirectional Spin Filter Using Quantum Coherence. *Science*, **299**, 679–682.
- Fujisawa, T., Austing, D. G., Tokura, Y., Hirayama, Y. and Tarucha, S. (2002). Allowed and forbidden transitions in artificial hydrogen and helium atoms. *Nature*, **419**, 278.
- Fujisawa, T., Hayashi, T. and Sasaki, S. (2006). Time-dependent single-electron transport through quantum dots. *Reports on Progress in Physics*, **69**, 759–796.
- Fujisawa, T., Tokura, Y. and Hirayama, Y. (2001). Transient current spectroscopy of a quantum dot in the Coulomb blockade regime. *Phys. Rev. B*, **63**, 081304.
- Giedke, G., Taylor, J. M., D’Alessandro, D., Lukin, M. D. and Imamoglu, A. (2005). Quantum measurement of the nuclear spin polarization in quantum dots. <http://arXiv.org/quant-ph/0508144>.
- Golden, J. M. and Halperin, B. I. (1996). Relation between barrier conductance and Coulomb blockade peak splitting for tunnel-coupled quantum dots. *Phys. Rev. B*, **53**, 3893–3900.
- Golovach, V. N. and Loss, D. (2004). Transport through a double quantum dot in the sequential- and co- tunneling regimes. *Phys. Rev. B*, **69**, 245327.
- Golovach, V. N., Borhani, M. and Loss, D. (2006). Electric dipole induced spin resonance in quantum dots. <http://arXiv.org/cond-mat/0601674>.
- Golovach, V. N., Khaetskii, A. and Loss, D. (2004). Phonon-induced decay of the electron spin in quantum dots. *Phys. Rev. Lett.*, **93**, 016601.
- Graeber, M. R., Coish, W. A., Hoffmann, C., Weiss, M., Furer, J., Oberholzer, S., Loss, D. and Schoenenberger, C. (2006). Molecular states in carbon nanotube double quantum dots. <http://arXiv.org/cond-mat/0603367>.
- Gywat, O., Burkard, G. and Loss, D. (2002). Biexcitons in coupled quantum dots as a source of entangled photons. *Phys. Rev. B*, **65**, 205329.
- Gywat, O., Engel, H.-A., Loss, D., Epstein, R. J., Mendoza, F. M. and Awschalom, D. D. (2004). Optical detection of single-electron spin decoherence in a quantum dot. *Phys. Rev. B*, **69**, 205303.
- Hanson, R. and Burkard, G. (2006). Universal set of quantum gates for double-dot spin qubits with fixed inter-dot coupling. <http://ArXiv.org/cond-mat/0605576>.

- Hanson, R., van Beveren, L. H. W., Vink, I. T., Elzerman, J. M., Naber, W. J. M., Koppens, F. H. L., Kouwenhoven, L. P. and Vandersypen, L. M. K. (2005). Single-shot readout of electron spin states in a quantum dot using spin-dependent tunnel rates. *Phys. Rev. Lett.*, **94**, 196802.
- Hanson, R., Vandersypen, L. M., van Beveren, L. H., Elzerman, J. M., Vink, I. T. and Kouwenhoven, L. P. (2004). Semiconductor few-electron quantum dot operated as a bipolar spin filter. *Phys. Rev. B*, **70**, 241304.
- Hanson, R., Witkamp, B., Vandersypen, L. M., van Beveren, L. H., Elzerman, J. M. and Kouwenhoven, L. P. (2003). Zeeman Energy and Spin Relaxation in a One-Electron Quantum Dot. *Phys. Rev. Lett.*, **91**, 196802.
- Hatano, T., Stopa, M. and Tarucha, S. (2005). Single-Electron Delocalization in Hybrid Vertical-Lateral Double Quantum Dots. *Science*, **309**, 268–271.
- Hayashi, T., Fujisawa, T., Cheong, H. D., Jeong, Y. H. and Hirayama, Y. (2003). Coherent manipulation of electronic states in a double quantum dot. *Phys. Rev. Lett.*, **91**, 226804.
- Hirjibehedin, C. F., Lutz, C. P. and Heinrich, A. J. (2006). Spin Coupling in Engineered Atomic Structures. *Science*, **312**, 1021–1024.
- Hohenester, U. (2004). Optical properties of semiconductor nanostructures: decoherence versus quantum control. <http://arXiv.org/cond-mat/0406346>.
- Hu, X. (2004). Spin-based quantum dot quantum computing. <http://arXiv.org/cond-mat/0411012>.
- Hu, X. and Das Sarma, S. (2006). Charge-Fluctuation-Induced Dephasing of Exchange-Coupled Spin Qubits. *Phys. Rev. Lett.*, **96**, 100501.
- Hüttel, A. K., Ludwig, S., Lorenz, H., Eberl, K. and Kotthaus, J. P. (2005). Direct control of the tunnel splitting in a one-electron double quantum dot. *Phys. Rev. B*, **72**, 081310.
- Hüttel, A. K., Weber, J., Holleitner, A. W., Weinmann, D., Eberl, K. and Blick, R. H. (2004). Nuclear spin relaxation probed by a single quantum dot. *Phys. Rev. B*, **69**, 073302.
- Imamoğlu, A., Awschalom, D. D., Burkard, G., DiVincenzo, D. P., Loss, D., Sherwin, M. and Small, A. (1999). Quantum Information Processing Using Quantum Dot Spins and Cavity QED. *Phys. Rev. Lett.*, **83**, 4204–4207.
- ITRS (2005). International technology roadmap for semiconductors. <http://public.itrs.net/>.
- Johnson, A. C., Petta, J. R., Marcus, C. M., Hanson, M. P. and Gossard, A. C. (2005). Singlet-triplet spin blockade and charge sensing in a few-electron double quantum dot. *Phys. Rev. B*, **72**, 165308.



- Johnson, A. C., Petta, J. R., Taylor, J. M., Yacoby, A., Lukin, M. D., Marcus, C. M., Hanson, M. P. and Gossard, A. C. (2005). Relaxation of single electron spins by nuclei in a double quantum dot. *Nature*, **435**, 925.
- Jouravlev, O. N. and Nazarov, Y. V. (2006). Electron Transport in a Double Quantum Dot governed by a Nuclear Magnetic Field. *Phys. Rev. Lett.*, **96**, 176804.
- Kato, Y., Myers, R. C., Gossard, A. C. and Awschalom, D. D. (2004). Coherent spin manipulation without magnetic fields in strained semiconductors. *Nature*, **427**, 50–53.
- Khaetskii, A. V. and Nazarov, Y. V. (2000). Spin relaxation in semiconductor quantum dots. *Phys. Rev. B*, **61**, 12639–12642.
- Khaetskii, A. V. and Nazarov, Y. V. (2001). Spin-flip transitions between Zeeman sublevels in semiconductor quantum dots. *Phys. Rev. B*, **64**, 125316.
- Khaetskii, A. V., Loss, D. and Glazman, L. (2002). Electron spin decoherence in quantum dots due to interaction with nuclei. *Phys. Rev. Lett.*, **88**, 186802.
- Klauser, D., Coish, W. A. and Loss, D. (2005). Nuclear spin state narrowing via gate-controlled Rabi oscillations in a double quantum dot. *Phys. Rev. B*, **73**, 205302.
- Klimeck, G., Chen, G. and Datta, S. (1994). Conductance spectroscopy in coupled quantum dots. *Phys. Rev. B*, **50**, 2316–2324.
- Koiller, B., Hu, X., Capaz, R. B., Martins, A. S. and Das Sarma, S. (2005). Silicon-based spin and charge quantum computation. *AN.ACAD.BRAS.CIENC.*, **77**, 201. <http://arXiv.org/cond-mat/0505169>.
- Koppens, F. H. L., Folk, J. A., Elzerman, J. M., Hanson, R., van Beveren, L. H. W., Vink, I. T., Tranitz, H. P., Wegscheider, W., Kouwenhoven, L. P. and Vandersypen, L. M. K. (2005). Control and Detection of Singlet-Triplet Mixing in a Random Nuclear Field. *Science*, **309**, 1346–1350.
- Koppens, F. H. L. et al. (2006). Driven coherent oscillations of a single electron spin in a quantum dot. *Unpublished*. (to appear in Nature).
- Kouwenhoven, L. P., Austing, D. G. and Tarucha, S. (2001). Few-electron quantum dots. *Reports on Progress in Physics*, **64**, 701–736.
- Kroutvar, M., Ducommun, Y., Heiss, D., Bichler, M., Schuh, D., Abstreiter, G. and Finley, J. J. (2004). Optically programmable electron spin memory using semiconductor quantum dots. *Nature*, **432**, 81.
- Laird, E. A., Petta, J. R., Johnson, A. C., Marcus, C. M., Yacoby, A., Hanson, M. P. and Gossard, A. C. (2005). Effect of exchange interaction on spin dephasing in a double quantum dot. <http://arXiv.org/cond-mat/0512077>.

- Lehmann, J. and Loss, D. (2006). Cotunneling current through quantum dots with phonon-assisted spin-flip processes. *Phys. Rev. B*, **73**, 045328.
- Lesovik, G. B., Martin, T. and Blatter, G. (2001). Electronic entanglement in the vicinity of a superconductor. *European Physical Journal B*, **24**, 287–290.
- Levitov, L. S. and Rashba, E. I. (2003). Dynamical spin-electric coupling in a quantum dot. *Phys. Rev. B*, **67**, 115324.
- Levy, J. (2002). Universal Quantum Computation with Spin-1/2 Pairs and Heisenberg Exchange. *Phys. Rev. Lett.*, **89**, 147902.
- Lidar, D. A. and Wu, L.-A. (2002). Reducing Constraints on Quantum Computer Design by Encoded Selective Recoupling. *Phys. Rev. Lett.*, **88**, 017905.
- Loss, D. and DiVincenzo, D. P. (1998). Quantum computation with quantum dots. *Phys. Rev. A*, **57**, 120.
- Loss, D. and Sukhorukov, E. V. (2000). Probing Entanglement and Nonlocality of Electrons in a Double-Dot via Transport and Noise. *Phys. Rev. Lett.*, **84**, 1035–1038.
- Lyanda-Geller, Y. B., Aleiner, I. L. and Altshuler, B. L. (2002). Coulomb "blockade" of nuclear spin relaxation in quantum dots. *Phys. Rev. Lett.*, **89**, 107602.
- Makhlin, Y., Schön, G. and Shnirman, A. (2001). Quantum-state engineering with Josephson-junction devices. *Rev. Mod. Phys.*, **73**, 357–400.
- Martin, I., Mozyrsky, D. and Jiang, H. W. (2003). A Scheme for Electrical Detection of Single-Electron Spin Resonance. *Physical Review Letters*, **90**, 018301.
- Mason, N., Biercuk, M. J. and Marcus, C. M. (2004). Local Gate Control of a Carbon Nanotube Double Quantum Dot. *Science*, **303**, 655–658.
- Meier, F., Levy, J. and Loss, D. (2003*a*). Quantum computing with antiferromagnetic spin clusters. *Phys. Rev. B*, **68**, 134417.
- Meier, F., Levy, J. and Loss, D. (2003*b*). Quantum computing with spin cluster qubits. *Phys. Rev. Lett.*, **90**, 047901.
- Mélin, R. (2001). Electronic EPR-like experiments with superconductors. <http://arXiv.org/cond-mat/0105073>.
- Merkulov, I. A., Efros, A. L. and Rosen, M. (2002). Electron spin relaxation by nuclei in semiconductor quantum dots. *Phys. Rev. B*, **65**, 205309.

- Myers, R. C., Ku, K. C., Li, X., Samarth, N. and Awschalom, D. D. (2005). Optoelectronic control of spin dynamics at near-terahertz frequencies in magnetically doped quantum wells. *Phys. Rev. B*, **72**, 041302(R).
- Ohno, Y., Young, D. K., Beschoten, B., Matsukura, F., Ohno, H. and Awschalom, D. D. (1999). Electrical spin injection in a ferromagnetic semiconductor heterostructure. *Nature*, **402**, 790–792.
- Oliver, W. D., Yamaguchi, F. and Yamamoto, Y. (2002). Electron Entanglement via a Quantum Dot. *Phys. Rev. Lett.*, **88**, 037901.
- Ono, K. and Tarucha, S. (2004). Nuclear-Spin-Induced Oscillatory Current in Spin-Blockaded Quantum Dots. *Phys. Rev. Lett.*, **92**, 256803.
- Ono, K., Austing, D. G., Tokura, Y. and Tarucha, S. (2002). Current Rectification by Pauli Exclusion in a Weakly Coupled Double Quantum Dot System. *Science*, **297**, 1313–1317.
- Ota, T., Rontani, M., Tarucha, S., Nakata, Y., Song, H. Z., Miyazawa, T., Usuki, T., Takatsu, M. and Yokoyama, N. (2005). Few-Electron Molecular States and Their Transitions in a Single InAs Quantum Dot Molecule. *Phys. Rev. Lett.*, **95**, 236801.
- Paget, D., Lampel, G., Sapoval, B. and Safarov, V. I. (1977). Low field electron-nuclear spin coupling in gallium arsenide under optical pumping conditions. *Phys. Rev. B*, **15**, 5780–5796.
- Pals, P. and MacKinnon, A. (1996). Coherent tunnelling through two quantum dots with Coulomb interaction. *Journal of the Physics of Condensed Matter*, **8**, 5401–5414.
- Petta, J. R., Johnson, A. C., Marcus, C. M., Hanson, M. P. and Gossard, A. C. (2004). Manipulation of a single charge in a double quantum dot. *Phys. Rev. Lett.*, **93**, 186802.
- Petta, J. R., Johnson, A. C., Taylor, J. M., Laird, E. A., Yacoby, A., Lukin, M. D., Marcus, C. M., Hanson, M. P. and Gossard, A. C. (2005). Coherent Manipulation of Coupled Electron Spins in Semiconductor Quantum Dots. *Science*, **309**, 2180–2184.
- Petta, J. R., Johnson, A. C., Yacoby, A., Marcus, C. M., Hanson, M. P. and Gossard, A. C. (2005). Pulsed-gate measurements of the singlet-triplet relaxation time in a two-electron double quantum dot. *Phys. Rev. B*, **72**, 161301.
- Pioro-Ladrière, M., Ciorga, M., Lapointe, J., Zawadzki, P., Korkusiński, M., Hawrylak, P. and Sachrajda, A. S. (2003). Spin-Blockade Spectroscopy of a Two-Level Artificial Molecule. *Phys. Rev. Lett.*, **91**, 026803.
- Potok, R. M., Folk, J. A., Marcus, C. M. and Umansky, V. (2002). Detecting Spin-Polarized Currents in Ballistic Nanostructures. *Phys. Rev. Lett.*, **89**, 266602.

- Prinz, G. A. (1998). Magnetoelectronics. *Science*, **282**, 1660–1663.
- Prinz, G. and Hathaway, K. (1995). Magnetoelectronics - special issue. *Physics Today*, **48**, 24–25.
- Rashba, E. I. and Efros, A. L. (2003). Orbital Mechanisms of Electron-Spin Manipulation by an Electric Field. *Phys. Rev. Lett.*, **91**, 126405.
- Raussendorf, R. and Briegel, H. (2001). A one-way quantum computer. *Phys. Rev. Lett.*, **86**, 5188–5191.
- Recher, P. and Loss, D. (2002). Superconductor coupled to two Luttinger liquids as an entangler for electron spins. *Phys. Rev. B*, **65**, 165327.
- Recher, P. and Loss, D. (2003). Dynamical Coulomb Blockade and Spin-Entangled Electrons. *Phys. Rev. Lett.*, **91**, 267003.
- Recher, P., Sukhorukov, E. V. and Loss, D. (2000). Quantum Dot as Spin Filter and Spin Memory. *Phys. Rev. Lett.*, **85**, 1962–1965.
- Recher, P., Sukhorukov, E. V. and Loss, D. (2001). Andreev tunneling, Coulomb blockade, and resonant transport of nonlocal spin-entangled electrons. *Phys. Rev. B*, **63**, 165314.
- Requist, R., Schliemann, J., Abanov, A. G. and Loss, D. (2005). Double occupancy errors in quantum computing operations: Corrections to adiabaticity. *Phys. Rev. B*, **71**, 115315.
- Salis, G., Kato, Y., Ensslin, K., Driscoll, D. C., Gossard, A. C. and Awschalom, D. D. (2001). Electrical control of spin coherence in semiconductor nanostructures. *Nature*, **414**, 619–622.
- Samuelsson, P., Sukhorukov, E. V. and Büttiker, M. (2004). Electrical current noise of a beamsplitter as a test of spin entanglement. *Phys. Rev. B*, **70**, 115330.
- Saraga, D. S., Altshuler, B. L., Loss, D. and Westervelt, R. M. (2004). Coulomb Scattering in a 2D Interacting Electron Gas and Production of EPR Pairs. *Phys. Rev. Lett.*, **92**, 246803.
- Saraga, D. S. and Loss, D. (2003). Spin-Entangled Currents Created by a Triple Quantum Dot. *Phys. Rev. Lett.*, **90**, 166803.
- Schaefer, H. and Strunz, W. T. (2005). Electron spin tomography through counting statistics: A quantum trajectory approach. *Phys. Rev. B*, **71**, 075321.
- Schedelbeck, G., Wegscheider, W., Bichler, M. and Abstreiter, G. (1997). Coupled quantum dots fabricated by cleaved edge overgrowth: From artificial atoms to molecules. *Science*, **278**, 1793.

- Schliemann, J., Khaetskii, A. and Loss, D. (2003). Electron spin dynamics in quantum dots and related nanostructures due to hyperfine interaction with nuclei. *J. Phys.: Condens. Matter*, **15**, R1809–R1833.
- Schliemann, J., Khaetskii, A. V. and Loss, D. (2002). Spin decay and quantum parallelism. *Phys. Rev. B*, **66**, 245303.
- Schliemann, J., Loss, D. and MacDonald, A. H. (2001). Double-occupancy errors, adiabaticity, and entanglement of spin qubits in quantum dots. *Phys. Rev. B*, **63**, 085311.
- Schmidt, T., Haug, R. J., Klitzing, K. V., Förster, A. and Lüth, H. (1997). Spectroscopy of the Single-Particle States of a Quantum-Dot Molecule. *Phys. Rev. Lett.*, **78**, 1544–1547.
- Shabaev, A., Efros, A., Gammon, D. and Merkulov, I. A. (2003). Optical readout and initialization of an electron spin in a single quantum dot. *Phys. Rev. B*, **68**, 201305(R).
- Shenvi, N., de Sousa, R. and Whaley, K. B. (2005a). Nonperturbative bounds on electron spin coherence times induced by hyperfine interactions. *Phys. Rev. B*, **71**, 144419.
- Shenvi, N., de Sousa, R. and Whaley, K. B. (2005b). Universal scaling of hyperfine-induced electron spin echo decay. *Phys. Rev. B*, **71**, 224411.
- Sleator, T. and Weinfurter, H. (1995). Realizable Universal Quantum Logic Gates. *Phys. Rev. Lett.*, **74**, 4087–4090.
- Slichter, C. P. (1980). *Principles of Magnetic Resonance*. Springer-Verlag, Berlin.
- Stepanenko, D. and Bonesteel, N. E. (2004). Universal Quantum Computation through Control of Spin-Orbit Coupling. *Phys. Rev. Lett.*, **93**, 140501.
- Stepanenko, D., Bonesteel, N. E., DiVincenzo, D. P., Burkard, G. and Loss, D. (2003). Spin-orbit coupling and time-reversal symmetry in quantum gates. *Phys. Rev. B*, **68**, 115306.
- Stepanenko, D., Burkard, G., Giedke, G. and Imamoglu, A. (2005). Enhancement of electron spin coherence by optical preparation of nuclear spins. *Phys. Rev. Lett.*, **96**, 136401.
- Stewart, D. R., Sprinzak, D., Marcus, C. M., Duruoz, C. I. and Harris, J. S., J. (1997). Correlations Between Ground and Excited State Spectra of a Quantum Dot. *Science*, **278**, 1784–1788.
- Stopa, M. and Marcus, C. M. (2006). Magnetic field control of exchange and noise immunity in double quantum dots. <http://arxiv.org/cond-mat/0604008>.

- Tarucha, S., Austing, D. G., Honda, T., van der Hage, R. J. and Kouwenhoven, L. P. (1996). Shell filling and spin effects in a few electron quantum dot. *Phys. Rev. Lett.*, **77**, 3613.
- Taylor, J. M., Engel, H. A., Dur, W., Yacoby, A., Marcus, C. M., Zoller, P. and Lukin, M. D. (2005). Fault-tolerant architecture for quantum computation using electrically controlled semiconductor spins. *Nat Phys*, **1**, 177–183.
- Taylor, J. M., Petta, J. R., Johnson, A. C., Yacoby, A., Marcus, C. M. and Lukin, M. D. (2006). Relaxation, dephasing, and quantum control of electron spins in double quantum dots. <http://arXiv.org/cond-mat/0602470>.
- Tokura, Y., van der Wiel, W. G., Obata, T. and Tarucha, S. (2006). Coherent Single Electron Spin Control in a Slanting Zeeman Field. *Phys. Rev. Lett.*, **96**, 047202.
- van der Wiel, W. G., de Franceschi, S., Elzerman, J. M., Fujisawa, T., Tarucha, S. and Kouwenhoven, L. P. (2003). Electron transport through double quantum dots. *Rev. Mod. Phys.*, **75**, 1–22.
- van der Wiel, W. G., Stopa, M., Kodera, T., Hatano, T. and Tarucha, S. (2006). Semiconductor quantum dots for electron spin qubits. *New Journal of Physics*, **8**, 28.
- Weinmann, D. (2003). Spin Blockades in the Transport through Quantum Dots. *LNP Vol. 630: Anderson Localization and Its Ramifications: Disorder, Phase Coherence and Electron Correlations*, **630**, 289–301.
- Weinmann, D., Häusler, W. and Kramer, B. (1995). Spin Blockades in Linear and Nonlinear Transport through Quantum Dots. *Phys. Rev. Lett.*, **74**, 984–987.
- Witzel, W. M., de Sousa, R. and Das Sarma, S. (2005). Quantum theory of spectral-diffusion-induced electron spin decoherence. *Phys. Rev. B*, **72**, 161306.
- Wolf, S. A., Awschalom, D. D., Buhrman, R. A., Daughton, J. M., von Molnár, S., Roukes, M. L., Chtchelkanova, A. Y. and Treger, D. M. (2001). Spintronics: A spin-based electronics vision for the future. *Science*, **294**, 1488–1495.
- Wu, L.-A., Lidar, D. A. and Friesen, M. (2004). One-Spin Quantum Logic Gates from Exchange Interactions and a Global Magnetic Field. *Phys. Rev. Lett.*, **93**, 030501.
- Wu, L., Byrd, M. and Lidar, D. (2002). Polynomial-Time Simulation of Pairing Models on a Quantum Computer. *Phys. Rev. Lett.*, **89**, 57904.
- Wu, L., Zanardi, P. and Lidar, D. (2005). Holonomic Quantum Computation in Decoherence-Free Subspaces. *Phys. Rev. Lett.*, **95**, 130501.

- Yao, W., Liu, R.-B. and Sham, L. J. (2005). Theory of electron spin decoherence by interacting nuclear spins in a quantum dot. <http://arXiv.org/cond-mat/0508441>.
- Yao, W., Liu, R.-B. and Sham, L. J. (2006). Restoring coherence lost to a mesoscopic bath. <http://arXiv.org/cond-mat/0604634>.
- Yuzbashyan, E. A., Altshuler, B. L., Kuznetsov, V. B. and Enolskii, V. Z. (2004). Solution for the dynamics of the bcs and central spin problems. [cond-mat/0407501](http://arXiv.org/cond-mat/0407501).
- Zener, C. (1932). Non-adiabatic crossing of energy levels. *Proceedings of the Royal Society of London*, **137**, 696.
- Ziegler, R., Bruder, C. and Schoeller, H. (2000). Transport through double quantum dots. *Phys. Rev. B*, **62**, 1961–1970.
- Zumbühl, D. M., Marcus, C. M., Hanson, M. P. and Gossard, A. C. (2004). Co-tunneling Spectroscopy in Few-Electron Quantum Dots. *Phys. Rev. Lett.*, **93**, 256801.